Functional analysis of two Arabidopsis COPII components, AtSec24B and AtSec24C, in gametogenesis

（配偶体形成における二種類のシロイヌナズナ COP Ⅱ 構成因子、AtSec24B 及び AtSec24C の機能解析）

Yuji Tanaka

田中　優史

2013

Contents

Abbreviation

A. thaliana	: *Arabidopsis thaliana*
A. tumefaciens	: *Agrobacterium tumefaciens*
cDNA	: complementary deoxyribonucleic acid
CDS	: coding sequence
CFP	: cyan fluorescent protein
CLSM	: confocal laser scanning microscope
COPII	: coat protein complex II
DAPI	: 4',6-diamidino-2-phenylindole
E. coli	: *Escherichia coli*
ER	: endoplasmic reticulum
ERES	: ER export site
GFP	: green fluorescent protein
GPT	: UDP-*N*-acetylglucosamine: dolichol phosphate *N*-acetylglucosamine-1-P transferase
GTP	: guanosine triphosphate
GUS	: β-glucuronidase
H. sapiens	: *Homo sapiens*
mRFP	: monomeric red fluorescent protein
mRNA	: messenger ribonucleic acid
MS	: Murashige and Skoog
M. musculus	: *Mus musculus*
O. sativa	: *Oryza sativa*
PCR	: polymerase chain reaction
PMII	: pollen mitosis II
P_{35S}	: cauliflower mosaic virus 35S promoter
Pnos	: nopaline synthase promoter
S. cerevisiae	: *Saccharomyces cerevisiae*
SEM	: scanning electron microscopy
SNARE	: soluble *N*-ethylmaleimide-sensitive factor attachment protein receptor
Tnos	: nopaline synthase terminator
T-DNA	: transfer deoxyribonucleic acid
WT	: wild-type

Chapter 1

Introduction

Arabidopsis thaliana

Arabidopsis thaliana is an annual flowering plant, and is often used as a model plant in molecular biology for the following reasons: (i) it is small size; (ii) culture is easy in laboratory; (iii) cross- and self-fertilization are easy; (iv) its generation time is rapid (approximately 5-6 weeks); (v) its genome is small (five chromosomes) and its DNA sequence had been already determined; (vi) mutagenesis and transformation are easy [1]. In addition, many transformants and mutants are maintained in the Arabidopsis Biological Resource Center (ABRC). Plant researchers can easily obtain the mutants and T-DNA inserted lines from the ABRC, which is a great advantage in using *A. thaliana* on plant research.

Vesicle transport

Eukaryotic cells have many organelles including the endomembrane system. The endomembrane system mainly composes of the endoplasmic reticulum (ER), the Golgi body, the endosome, and the vesicle in plant. They involves in export of secretion protein and membrane proteins, import of extracellular materials, and accumulation of lipids and proteins. Membrane compartments composing the system are independent on each other and possess specific function. The function of the compartments is determined by involved enzymes and proteins. The composition of the proteins in the compartments is maintained by selective protein transport mediated by transport vesicles. The transport vesicles are composed of single-layer membrane covered with coat protein complexes, and are generated from donor membrane by assembly of the coat proteins. Some of the coat proteins are involved in selection of proteins that is destined for incorporation into the vesicle. Three types of coat protein complexes are well-known: coat protein complex I (COPI), coat protein complex II (COPII), and clathrin coat complex (Figure 1-1). The COPI-coated vesicles mediate protein transport from Golgi apparatus to ER and internal transport between Golgi cisternae. The clathrin coat vesicles are involved in post-Golgi transport and endocytosis. The COPII-coated vesicles (COPII vesicle) mediate protein transport from ER to Golgi apparatus.

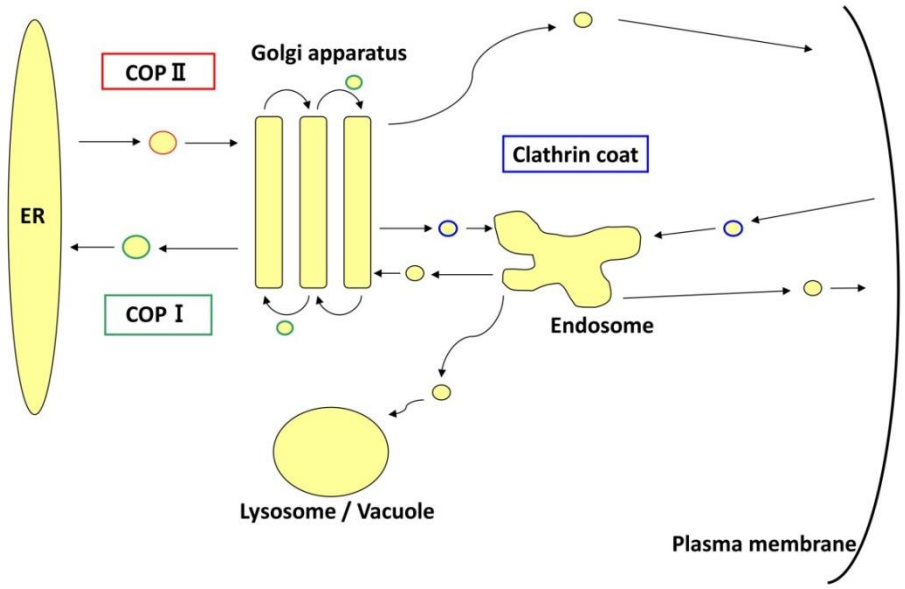

Fig. 1-1 Intracellular vesicle transport and coat protein complexes
The COPI-coated vesicles mediate protein transport from Golgi to ER and internal transport between Golgi cisternae (green). The COPII-coated vesicles mediate protein transport from ER to Golgi (red). The clathrin coat vesicles are involved in post-Golgi transport and endocytosis (blue). [cited from Sato K. and Nakano A. (2007) *FEBS Letters* 581 2076-2082.]

COPII vesicle and Sec24

Proteins synthesized on ER membrane are transported into the destined membrane compartments or extracellular space. Most of such proteins are first loaded into the COPII vesicles. In *Saccharomyces cerevisiae*, the COPII vesicle formation requires small GTP-binding protein Sar1p and two coat protein complexes (Sec23/24p and Sec13/31p) [2] and is achieved by continuous assembly of these coat proteins [3] (Figure 1-2). In this process, Sar1p acts as target molecule for recruitment of other COPII coat component onto the ER membrane. When Sar1p is activated by the Sar1p-specific guanine nucleotide exchange factor Sec12p that localized in the ER membrane, Sar1p is concurrently anchored into ER membrane via its N-terminal helical domain [4]. Sec23/24p complex is recruited from cytoplasm onto ER membrane to form a "prebudding complex" and captures cargo proteins destined for incorporation into the COPII vesicle. Sec13/31p complex concentrates the cargo into the COPII vesicle by cross-linking the adjacent prebudding complexes, which leads the vesicle budding to finish. This assembly of these coat proteins occurs

on the specialized ER subdomains, which are termed ER export site (ERES), to export proteins to the Golgi.

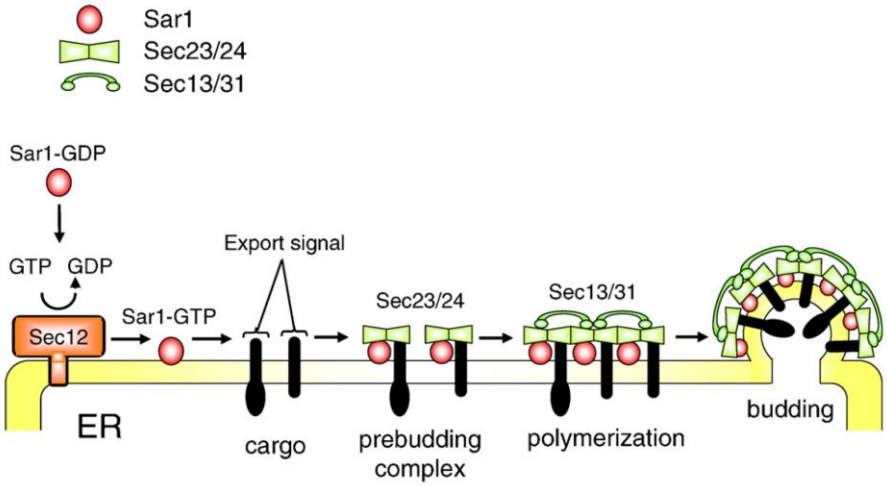

Fig. 1-2 COPII vesicle formation
The COPII vesicle formation is achieved by continuous assembly of small GTP-binding protein Sar1p and two coat protein complexes (Sec23/24p and Sec13/31p). [cited from Sato K. and Nakano A. (2007) *FEBS Letters* 581 2076-2082.]

Of the COPII, Sec24 possesses three cargo binding sites (A-, B-, and C-sites) for association with ER export signals included in cargo [5,6] (Figure 1-3), which contributes to selective protein transport by the transport vesicle. The Sec24 have similar tertiary structures to Sec23 [7] and form a bow-tie shaped heterodimer with Sec23 [8]. Because a cargo, Sec22, interacts to interface of Sec23/24 complex [9], the formation of dimer might be also important for the capture of cargo proteins.

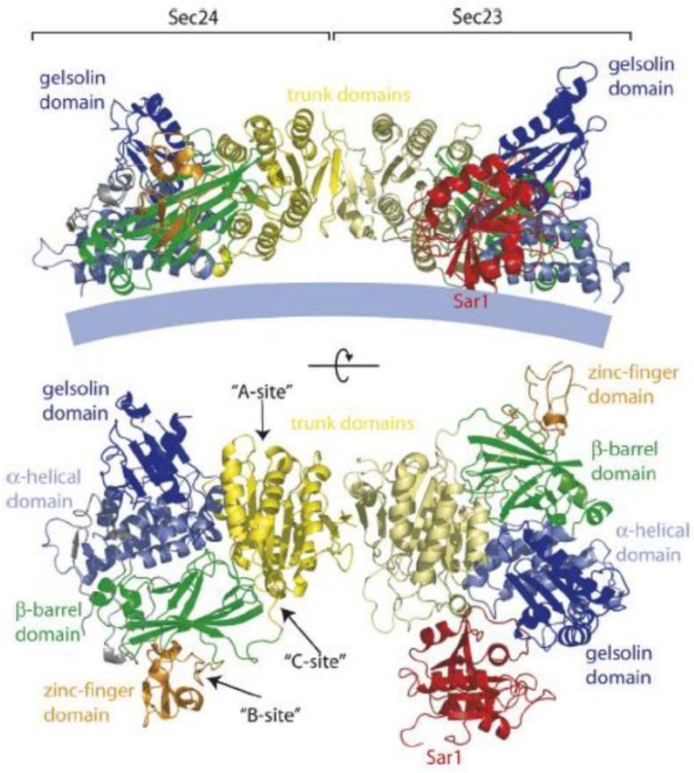

Fig. 1-3 Structure and domain of the Sec23/24p complex
The Sec23 and Sec24 have similar tertiary structures and form a bow-tie shaped heterodimer. Sec24 possesses three cargo binding sites (A-, B-, and C-sites) for association with cargo. [cited from Lee M.C.S. and Miller E.A. (2007) *Seminars in Cell & Developmental Biology* 18 424-434.]

Formation of gametophytes in *Arabidopsis thaliana* [10-12]

The male gametophyte (pollen) is formed from a diploid cell, microsporocyte, in the anther (Figure 1-4). The microsporocyte covered with callose wall undergoes meiosis to generate a tetrad which is an aggregate of four haploid cells, microspores, confined in the callose wall. The microspores are released from the tetrad after dissolution of the callose wall. The released microspore develops vacuole to force the microspore nucleus to migrate to a corner in the cell. After the migration, the microspore undergoes the first mitosis (pollen mitosis I) to produce a vegetative nucleus and a generative nucleus. Then the microspore is divided into a large vegetative cell and a small generative cell covered with the hemispherical cell wall. The generative cell migrates into the vegetative cell. At this time, the vacuole has split into smaller one and the hemispherical cell wall has been decomposed. The generative cell divides into two sperm cells in the vegetative cell (pollen mitosis II) and the microspore becomes mature pollen. After pollination, the mature pollen grows a pollen tube to transport the sperm cells to female gametophyte.

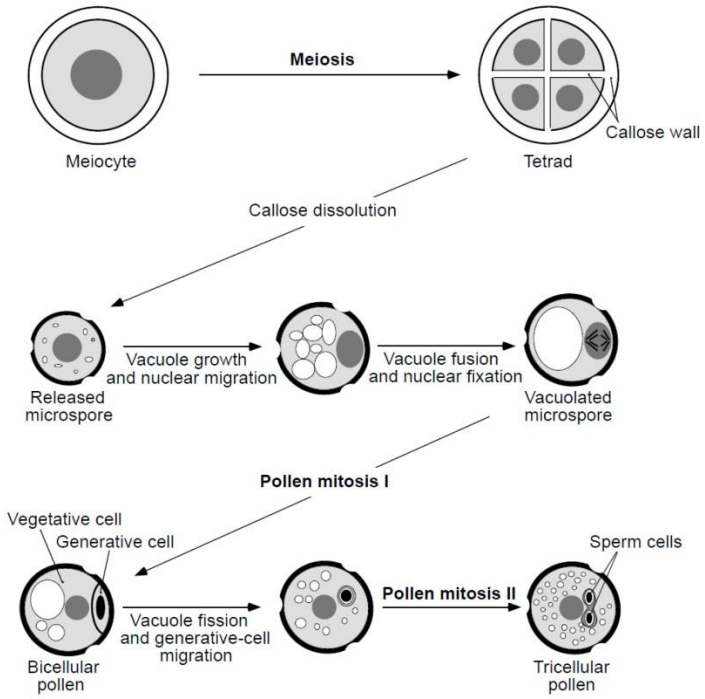

Fig. 1-4 Formation of male gametophyte in *A. thaliana*
The microspore undergoes two rounds of mitosis after meiosis and grows into mature pollen. [cited from Twell D., Park S.K., *et al.* (1998) *Trend in Plant Science* 3 305-310.]

Female gametophyte (embryo sac) is a monosporic embryo sac undergoing *Polygonum*-type megagametogenesis in *A. thaliana*. The embryo sac is formed from a megaspore mother cell (MMC) (Figure 1-5). The MMC undergoes meiosis to generate four megaspores. A functional megaspore grows and the other megaspores degenerate. The functional megaspore undergoes three rounds of mitosis without cytokinesis to produce an eight-nucleate coenocyte. After migration of two polar nuclei to the center of the coenocyte, the megaspore undergoes cellularization. The polar nucleus fuses with another polar nucleus, by which a secondary nucleus is generated. The embryo sac has seven cells (one central cell, three antipodal cells, two synergid cells, and one egg cell) with seven nuclei. As the embryo sac develops, the antipodal cells degenerate. The seven-celled embryo sac eventually develops into a four-celled mature embryo sac.

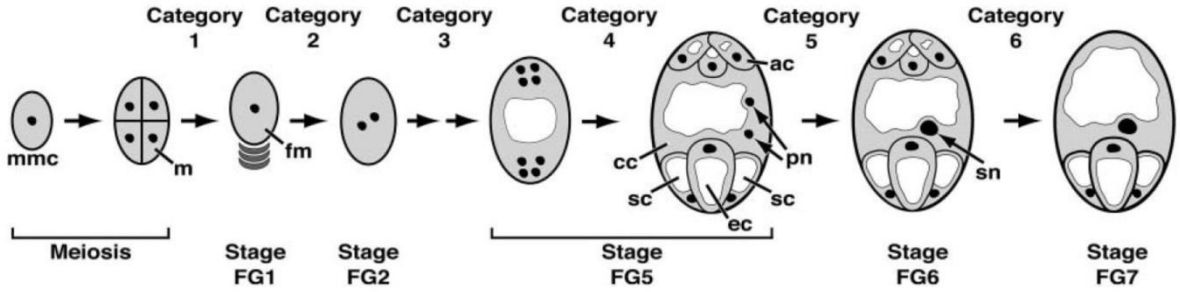

Fig. 1-5 Formation of female gametophyte in *A. thaliana*
The megaspore undergoes three rounds of mitosis without cytokinesis after meiosis. After the cellularization, the fusion of polar nuclei, and the degeneration of the antipodal cells, the megaspore develops into the four-celled embryo sac. ac: antipodal cell, cc: central cell, ec: egg cell, fm: functional megaspore, m: megaspore, mmc: megaspore mother cell, pn; polar nucleus, sn: secondary nucleus. [cited from Yadegari R. and Drews G.N. (2004) *The Plant Cell* 16 S133-S141.]

Gateway® recombination cloning technology [13]

Gateway® recombination cloning technology is application of site-specific recombination between phage λ and *Escherichia coli* genomes (Figure 1-6). Phage λ uses *att*P site on its genome and *att*B site on *E. coli* genome for insertion of the phage genome into the bacterial genome. The recombination between *att*P and *att*B sites needs the phage enzyme, integrase, (Int) and the bacterial protein, integration host factor (IHF). By the recombination of *att*P and *att*B sites, the phage genome is integrated into the bacterial genome and is flanked by *att*L and *att*R sites generated by this recombination. On the other hand, the *att*L and *att*R sites are used for excision of the phage genome from the bacterial genome, which needs Int, IHF, and an additional phage enzyme, excisionase (Xis). In this technology, the recombination reactions between *att*P and *att*B sites and between *att*L and *att*R sites are called BP reaction and LR reaction, respectively. Life Technology (Carlsbad, CA, USA) provides mixture of Int and IHF as BP clonase and that of Int, IHF, and Xis as LR clonase.

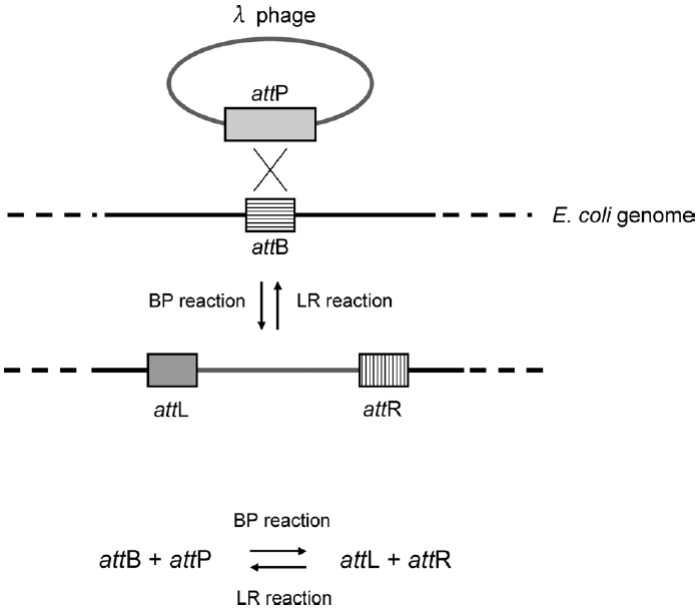

Fig. 1-6 The site-specific recombination between phage λ and *E. coli* genome
The *att*P site on the phage λ genome recombines the *att*B site on *E. coli* genome (BP reaction) in integration of the phage genome. When the phage genome is excised, *att*L and *att*R sites are recombined (LR reaction). [cited from Nakagawa T., Ishiguro S., *et al.* (2009) *Plant Biotechnology* 26 275-284.]

In a simple Gateway cloning system, four pairs of modified *att* sites are used. They are *att*B1 and *att*B2, *att*P1 and *att*P2, *att*L1 and *att*L2, and *att*R1 and *att*R2. Their recombination partner is restricted as follows: *att*B1 and *att*P1, *att*B2 and *att*P2, *att*L1 and *att*R1, and *att*L2 and *att*R2. To make an expression clone using the system, the *att*L and *att*R sites are inserted into an entry clone and a Destination vector, respectively. The entry clone carries an *att*L1-*gene*-*att*L2 construct and the Destination vector possesses a Gateway acceptable cassette including *att*R1 and *att*R2 sites between a promoter sequence and a transcriptional terminator as shown in Figure 1-7. By the LR reaction between the entry clone and the Destination vector, the "*gene*" sequence is cloned into the Destination vector and the expression clone is generated. At this time, *att*L sites on the entry clone are recombined into *att*P sites and *att*R sites on the Destination vector are recombined into *att*B sites.

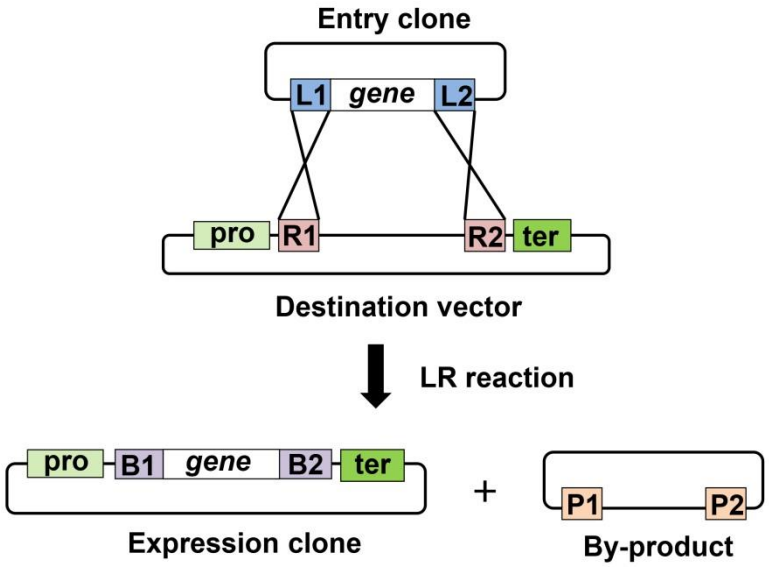

Fig. 1-7 The simple Gateway cloning with an entry clone and a Destination vector
The *att*L and *att*R sites are recombined and the DNA fragment, "*gene*", is introduced into the Destination vector with maintaining its orientation. B1: *att*B1, B2: *att*B2, L1: *att*L1, L2: *att*L2, P1: *att*P1, P2: *att*P2, R1: *att*R1, R2: *att*R2, pro: promoter, ter: transcriptional terminator

This system using Gateway technology has some advantages to achieve rapid construction of expression clones. First, a DNA fragment introduced into a Destination vector is maintained its orientation because the recombination of *att* sites is strictly regulated the partner *att* sites. Secondly, this cloning system does not need the restriction enzymes or the ligation and is not limited by existence of the enzyme sites in the DNA fragment. Thirdly, many Destination vectors have been developed for various hosts and for various purposes. Destination vectors for *E. coli*, yeast, insects, plants, and mammal cells are available. The vectors for expressing protein fused with tags or reporters have also been developed.

Gateway binary vector, pGWB and R4pGWB [14-16]

pGWB is Gateway compatible Destination vector series constructed by Dr. Tsuyoshi Nakagawa *et al.* for plant transformation. Because the pGWB possesses the replication origins for *E. coli* and *Agrobacterium tumefaciens*, it is available for gene transfer mediated by *A. tumefaciens* into plant genome. pGWB carries the *att*R1-*att*R2 type of Gateway acceptable cassette as shown

in Figure 1-7. In the pGWB, 16 kinds of reporter and epitope tag [synthetic green fluorescent protein (sGFP), hexahistidine tag (6xHis), FLAG-tag (FLAG), triple HA tag (3xHA), four repeats of the Myc tag (4xMyc), 10 repeats of the Myc tag (10xMyc), glutathione S-transferase (GST), T7-epitope tag (T7), tandem affinity purification (TAP), β-glucuronidase (GUS), modified luciferase (LUC), enhanced yellow fluorescent protein (EYFP), enhanced cyan fluorescent protein (ECFP), G3 green fluorescent protein (G3GFP), monomeric red fluorescent protein (mRFP), tag red fluorescent protein (TagRFP)] are available and can be added on either N-terminus or C-terminus of a protein desired to express. pGWB is suitable to promoter:repoter assay and overexpression of a fusion protein. Primitive pGWB possess two selection markers for kanamycin and hygormycin. Improved pGWB that is smaller size than the primitive pGWB carries a selection marker either for kanamycin, hygormycin, or BASTA®.

R4pGWB has been developed to easily construct clones enabling to express a protein under the desired promoter. The R4pGWB possesses a *att*R4-*att*R2 type of Gateway acceptable cassette (Figure 1-8). For construction of expression clone with this series, another entry clone carrying *att*L4-*promoter*-*att*R1 construct is used in addition to the gene entry clone (*att*L1-*gene*-*att*L2) shown in Figure 1-7. Because the *att*L4 site recombines with the only *att*R4 site, the "*promoter*" and "*gene*" sequence of the entry clones are introduced into an R4pGWB Destination vector as shown in Figure 1-8. In the R4pGWB, the same kinds of reporter/tag as that in pGWB are available. R4pGWB carries a selection marker either for kanamycin, hygormycin, or BASTA®.

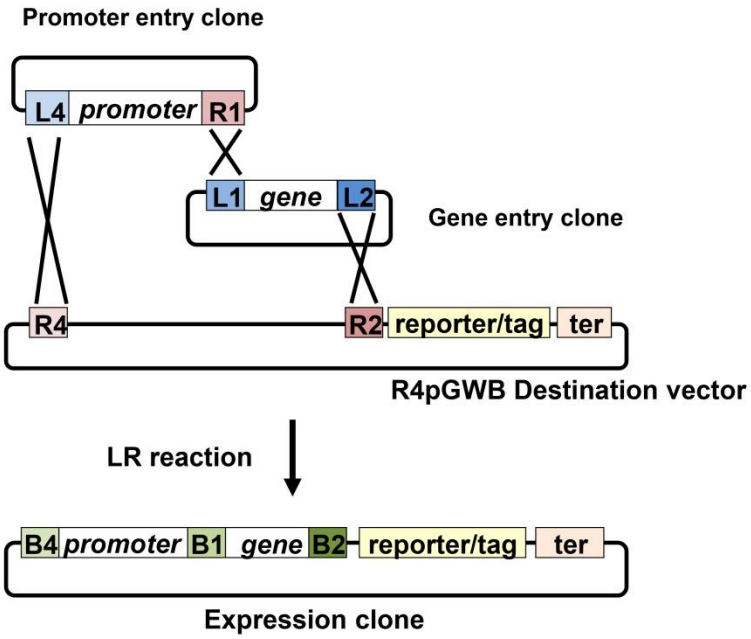

Fig. 1-8 Construction for an expression clone with R4pGWB Destination vector
The *att*L and *att*R sites are recombined and DNA fragments, "*promoter*" and "*gene*", are introduced into the R4pGWB Destination vector. B1: *att*B1, B2: *att*B2, B4: *att*B4, L1: *att*L1, L2: *att*L2, L4: *att*L4, R1: *att*R1, R2: *att*R2, R4: *att*R4, ter: transcriptional terminator

Tunicamycin and UDP-*N*-acetylglucosamine: dolichol phosphate *N*-acetylglucosamine-1-P transferase (GPT)

The protein glycosylation is important for polypeptide folding and multimer formation of proteins and protein export from ER. GPT catalyzes transference of *N*-acetylglucosamine-1-phosphate from UDP-*N*-acetylglucosamine to dolichol phosphate to form *N*-acetylglucosaminylpyrophosphoryl-dolichol [17] (Figure 1-9a), which is the first step for synthesis of *N*-linked glycoprotein in ER (Figure 1-10). Tunicamycin is complex of homologous nucleoside antibiotics produced by *Streptomyces lysosuperficus* [18] (Figure 1-9b) and blocks the synthesis of the glycoproteins by inhibiting the catalytic activity of GTP. Tunicamycin is used as a valuable tool for analysis of the above biological activities.

a

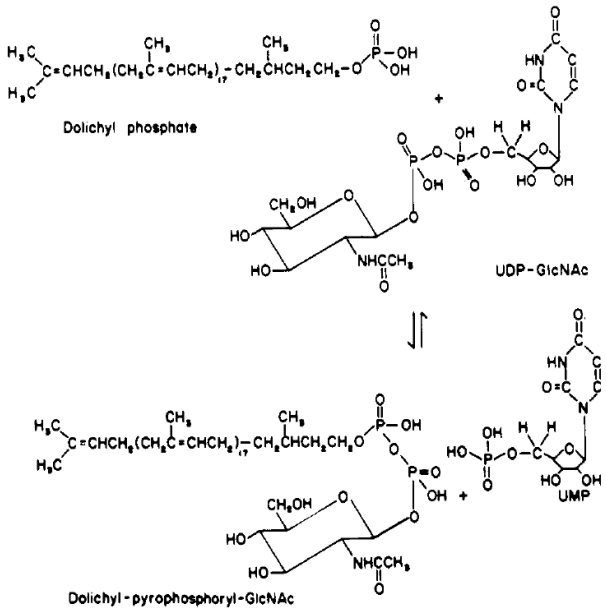

b

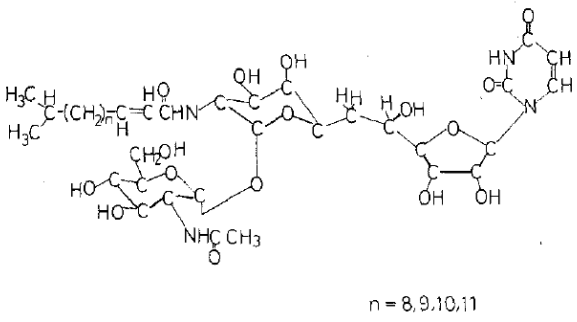

Fig. 1-9 The transference reaction of *N*-acetylglucosamine-1-phosphate to dolichol phosphate and the structure of tunicamycin

a The GTP catalyzes a reversible transference reaction of *N*-acetylglucosamine-1-phosphate between UDP-*N*-acetylglucosamine and *N*-acetylglucosaminylpyrophosphoryl-dolichol. [cited from Heifetz A., Keenan R.W., *et al.* (1979) *Biochemistry* 18 (11) 2186-2192]

b The structure of tunicamycin is similar to that of *N*-acetylglucosaminylpyrophosphoryl-dolichol. [cited from Takatsuki A., Kawamura K., *et al.* (1977) *Agricultural and Biological Chemistry* 41 (11) 2307-2309]

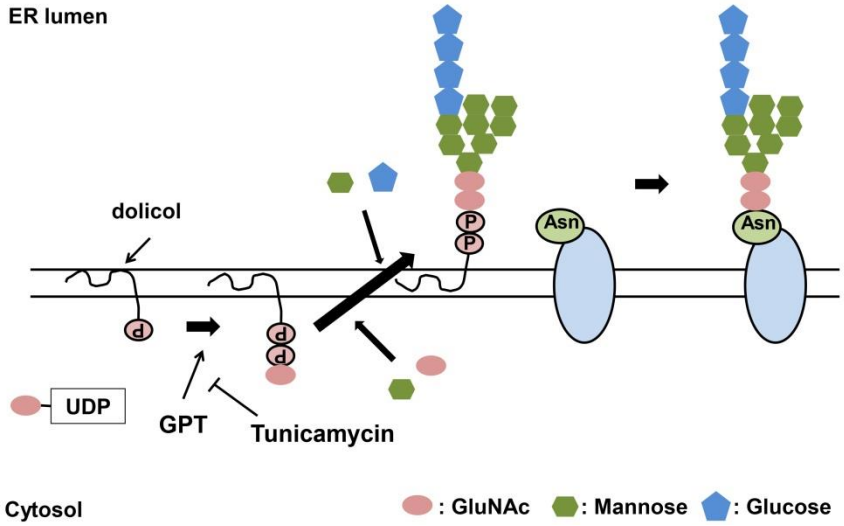

Fig. 1-10 The point of action for GTP and tunicamycin in protein glycosylation
The *N*-linked oligosaccharide is synthesized on carrier lipid, dolicol, and is added to asparagine side chain of protein. The GTP catalyzes the first step in the synthesis reaction of the oligosaccharide. The tunicamycin inhibits the catalysis of the GTP. Asn: asparagine, GluNAc: *N*-acetylglucosamine, P: phosphate group

Chapter 2

Redundant function of two Arabidopsis COPII components, AtSec24B and AtSec24C, is essential for male and female gametogenesis

Introduction

Eukaryotic cells use a vesicle transport system for intracellular protein trafficking. This system enables the protein transport between organelles by the following procedure. A donor membrane compartment releases small membrane vesicles as carriers of cargo proteins, and these vesicles fuse with and thereby import the cargo proteins into an accepter membrane compartment. Vesicle budding is driven by recruitment and assembly of coat proteins from the cytoplasm onto donor membrane. The coat protein complex deforms the membrane and also selects and concentrates cargo proteins into the vesicle.

Anterograde transport from the ER to the Golgi apparatus, the start of the secretory pathway, is mediated by COPII vesicles [19]. In *S. cerevisiae*, COPII vesicle formation requires the small GTP-binding protein Sar1p and two coat protein complexes (Sec23/24p and Sec13/31p), as shown by *in vitro* reconstitution assays using synthetic liposomes [2], and is achieved by continuous assembly of these coat proteins. In this process, Sar1p acts as a target molecule for the recruitment of other COPII components onto the ER membrane. Sar1p is activated by the Sar1p-specific guanine nucleotide exchange factor Sec12p, which localizes in the ER membrane [20-22]. Activated Sar1p is concurrently anchored into the ER membrane via its N-terminal helical domain [4], thereby restricting the subsequent assembly of COPII components onto the ER membrane. The Sec23/24p complex is recruited from the cytoplasm by Sar1p to form a “prebudding complex” and captures cargoes that are destined to be incorporated into COPII vesicle [23]. The Sec13/31p complex concentrates cargo into COPII vesicles by cross-linking the adjacent prebudding complexes, which leads to the completion of vesicle budding [3].

The Sec23/24p complex is a bow-tie shaped heterodimer of Sec23p and Sec24p; it forms the inner layer of the COPII coat with Sar1p [8]. Although Sec23p and Sec24p have similar tertiary structures and the same five domains [7], their function in COPII vesicles is different. Sec23p directly associates with Sar1p to act as a Sar1p-specific GTPase-activating protein [24]. Sec24p is thought to recognize cargo that is destined for incorporation into the vesicle [25]. The *S. cerevisiae* genome encodes two other isoforms of Sec24 in addition to Sec24p, called Iss1p and Lst1p. All three Sec24 paralogs select cargo via direct interaction between their cargo binding sites and the ER export

signals of the cargoes [5,6]. For example, the NPF motif and LxxME sequence of the *cis*-Golgi t-SNARE Sed5p bind to the A-site and the B-site of Sec24p, respectively [26].

In plant cells, molecular events driving ER-to-Golgi transport are well characterized on a cellular level. Biochemical and imaging analyses show that the GTPase function of Sar1 is controlled by Sec12 and is involved in ER-to-Golgi transport [27,28]. Live cell imaging using tobacco (*Nicotiana tabacum*) and *A. thaliana* suspension cultured cells demonstrate that several plant homologs of yeast COPII components, including Sec24p, are localized at ERES, which are specialized ER subdomains involved in protein export to the Golgi apparatus [29-31]. Overexpression of the Sec24 homolog increases the localization of the Sec13 homolog at ERES [32]. These reports indicate that vesicle formation by sequential association of COPII components is conserved in higher plants. Chloroplasts appear to possess a vesicle transport system that transports lipids synthesized in the chloroplast envelope membrane to the thylakoid membrane [33]. A bioinformatics analysis using subcellular localization prediction tools predicts that homologs of the COPII components are present in the chloroplasts [34].

Plant cells appear to use a similar mechanism for cargo selection by Sec24 as that of budding yeast. In an experiment using tobacco cells, overexpression of membrane cargo proteins promotes the accumulation a fusion construct of fluorescent protein and AtSec24A (one of three Sec24p homologs in *A. thaliana*) to ERES, and this accumulation is dependent on a functional ER export signal of cargoes [35]. Fluorescence resonance energy transfer measurements in *Vicia faba* guard cells indicate that the plant K^+-channel KAT1, which has a di-acidic ER export signal, interacts with AtSec24A in a signal-dependent manner [36]. Mutation of the amino acid residue of AtSec24A that corresponds to the arginine necessary for cargo binding in the B-site of yeast Sec24p causes abnormal ER morphology and organelle distribution in *A. thaliana* [37,38]. The sorting of cargo by AtSec24A appears to be involved in the maintenance of ER morphology and organelle distribution in *A. thaliana*. Recently, a study using a knockout line of *AtSec24A* indicates that the lack of AtSec24A leads to a reduction of pollen germination [39].

A. thaliana has three Sec24 homologs (denoted AtSec24s), and only AtSec24A has been characterized. To expand knowledge of the biological functions of AtSec24s in plant development, the author isolated T-DNA

insertion plants of *AtSec24B* and *AtSec24C* and examined the phenotypes of these mutants. Here, the author reports that AtSec24B contributes to pollen germination, whereas AtSec24B and AtSec24C are redundantly involved in gametophyte development. The author also reports the expression pattern and subcellular localizations of AtSec24s. These results indicate the importance of the function of AtSec24s in plant reproductive cells.

Material and methods

Plant materials and growth condition

Wild-type (WT) plants were *A. thaliana* Columbia (Col-0) distributed by ABRC (Ohio, USA). T-DNA insertion plants of AtSec24B (SALK_013076/*atsec24b-1*) and AtSec24C (SALK_001648/*atsec24c-1*) were obtained from the ABRC. For tetrad analysis using *quartet1* (*qrt1*) mutant, *qrt1-2* allele (CS8846) mutagenized by fast neutron was distributed from the ABRC. The seeds were surface sterilized and sowed on either Murashige and Skoog (MS) medium containing 0.8% (w/v) agar, MS salts, 1% (w/v) sucrose, and 0.01% (w/v) myo-inositol or Jiffy-7 (Jiffy Preforma Production K.K, Yokohama, Japan). Sowed seeds were incubated at 4°C for 2 days to vernalize and grown at 22°C under a light cycle of 16-h light/8-h dark or continuous light. The insertion of T-DNA was confirmed by PCR with the following primers shown in Table 2-1: *AtSec24B*-F and *atsec24b*-R for *AtSec24B*, *atsec24c*-F and *atsec24c*-R for *AtSec24C* and T-DNA-LB as a common primer to detect T-DNA.

Preparation of RNA and RT-PCR

Total RNAs were isolated from each organ in WT plants and cDNAs were synthesized with oligo-dT primer using ReverTraAce (TOYOBO, Osaka, Japan). PCR was performed with 25 cycles (*AtSec24A* and *Actin2*) or 30 cycles (*AtSec24B* and *AtSec24C*) using cDNA from each organ as a template with the following specific primers shown in Table 2-1: *AtSec24A*-F and *AtSec24A*-R for *AtSec24A*, *AtSec24B*-F and *AtSec24B*-R for *AtSec24B*, *AtSec24C*-F and

AtSec24C-R for *AtSec24C*, and *ACT2*-F and *ACT2*-R for *Actin2*.

Construction of entry clones for Gateway cloning

To construct promoter entry clones of *AtSec24A*, *AtSec24B*, and *AtSec24C*, the adenine of the translation initiation codon was designated as +1 and approximately 2 kbp upstream region were used as promoter of each *AtSec24*: -2215 to -1 for *AtSec24A*, -2433 to -1 for *AtSec24B*, and -2198 to -1 for *AtSec24C*. These regions were amplified from genomic DNA by adapter PCR with the corresponding *AtSec24s-pro-att*B1 and *AtSec24s-pro-att*B2 primers (Table 2-1). The resulting fragments were cloned into pDONR201 (Life Technologies) by a BP reaction according to the manufacturer's instructions (Life Technologies) to construct pDONR201-$Pro_{AtSec24s}$ (*att*L1-*AtSec24s promoter-att*L2) entry clones. pDONRP4-P1R-$Pro_{AtSec24B}$ (*att*L4-*AtSec24B promoter-att*R1) entry clones was also generated using pDONRP4-P1R (Life Technologies) with *AtSec24B-pro-att*B4 and *AtSec24B-pro-att*B1r primers (Table 2-1).

To construct coding sequence (CDS) entry clones of *AtSec24A*, *AtSec24B*, and *AtSec24C*, CDSs were amplified from the RIKEN Arabidopsis Full-Length cDNA (resource number: pda09694) provided by the RIKEN (http://www.brc.riken.jp/lab/epd/catalog/cdnaclone.html) for *AtSec24A*, and cDNA prepared from inflorescence RNA of WT for *AtSec24B* and *AtSec24C* by adapter PCR with *AtSec24s-att*B1 and *AtSec24s-att*B2 primers (Table 2-1). The CDS of SYP31 was amplified from pENTR-35S-SYP31 donated by Dr. Takashi Ueda (The University of Tokyo) by adapter PCR with *SYP31-att*B1 and *SYP31-att*B2 primers (Table 2-1). Amplified fragments were cloned into pDONR201 (Life Technologies) by the BP reaction to construct pDONR201-*AtSec24s* entry clones (*att*L1-*AtSec24s-att*L2) and the pDONR201-*SYP31* entry clone (*att*L1-*SYP31-att*L2).

Promoter:GUS constructs and histochemical analysis

pDONR201-$Pro_{AtSec24s}$ entry clones were introduced into the binary vector pGWB233 [40] by an LR reaction following the manufacturer's instructions

(Life Technologies) to generate *AtSec24s promoter:GUS* constructs. These constructs were introduced into *Agrobacterium tumefaciens* C58C1 (pMP90) and used to transform WT plants by the floral dip procedure [41]. Transformants were selected on MS medium containing 30 mg L^{-1} kanamycin and 100 mg L^{-1} Cefotax (Chugai Pharmaceutical Co., Tokyo, Japan). GUS staining was performed on whole seedlings and dissected plant organs from T_2 or T_3 lines of each construct and staining was observed as previously reported [42].

Subcellular localization analysis

For transient expression of AtSec24s-green fluorescent protein (GFP) under the control of the Cauliflower mosaic virus 35S promoter (P_{35S}), pDONR201-*AtSec24s* entry clones were introduced into pUGW51 [43] by the LR reaction to generate pUGW51-*AtSec24s*. To construct the SYP31- mRFP, pDONR201-*SYP31* was introduced into pUGW54 [43] to generate pUGW54-*SYP31*. pUGW51-*AtSec24s* and pUGW54-*SYP31* were mixed at a ratio of 4:1 and introduced into leaf epidermal cells of WT plants by particle bombardment as previously described [40], in which the helium pressure was 4.5 kgf cm^{-2} under a vacuum of 80 kPa. Following bombardment, the agar plate was filled with water to prevent desiccation. After incubation overnight at 22°C in the dark, leaves were viewed with a TCS SP5 confocal laser scanning microscopy (CLSM) (Leica Microsystems, Wetzlar, Germany) using an HCX PL APO CS 63.0x1.20 WATER UV objective lens. The GFP and mRFP were exited with the argon laser line (488 nm) and the helium-neon laser line (543 nm), respectively. The fluorescence of GFP and mRFP were detected at 500-530 nm and at 555-650 nm, respectively. Images were processed with Photoshop CS6 (Adobe Systems, San Jose, CA, USA).

In vitro pollen germination assay

To construct the *AtSec24B promoter:AtSec24B-GFP* expression clone, pDONRP4-P1R-$Pro_{AtSec24B}$ and pDONR201-*AtSec24B* entry clones were cloned into a binary vector R4pGWB550 [15] by the LR reaction. The resulting

construct was transformed into homozygous *atsec24b-1* plants and transformants were selected on MS medium containing 20 mg L^{-1} hygromycin B and 100 mg L^{-1} Cefotax (Chugai Pharmaceutical Co.). A T_2 line was used with WT, *atsec24b-1* and *atsec24c-1* plants for the *in vitro* pollen germination test, which was performed as previously described [44]. After incubation to allow pollen germination, the slides were observed and photographed with a SZX16 stereoscopic microscope (Olympus, Tokyo, Japan). More than 500 pollen grains were counted with ImageJ software (http://rsbweb.nih.gov/ij/) to calculate the rate of germination in each slide.

Light and electron microscopy for gametophyte analysis

For scanning electron microscopy (SEM), pollen tetrads from open flowers were mounted on carbon tape stuck on the specimen stub and coated with platinum/palladium. The specimens were observed using an S-4800 field emission SEM (Hitachi High-Tech, Tokyo, Japan). Approximately 100 pollen tetrads were categorized according to the number of normal pollen grains included in the tetrads and counted by ImageJ software to calculate the percentages of each type of pollen tetrads. The measurement was independently performed two and three times in each line. Alexander staining was performed as described on the website of an EMBO practical course (http://www.isv.cnrs-gif.fr/embo99/manuals/pdf/ch1.pdf). Pollen isolated from flowers at various developmental stages in an inflorescence was carefully extracted in 1 µg mL^{-1} 4',6-diamidino-2-phenylindole (DAPI) solution [45] on grass slides. The stained pollen was observed using a BX51 fluorescence microscope (Olympus) or a TCS SP5 CLSM (Leica Microsystems). Classification of developmental stages was defined according to the number of nuclei in microspores from each flower. If binuclear and trinuclear microspores coexisted in microspore tetrads from a flower, the developmental stage was classified as pollen mitosis II (PMII) stage. To observe the morphology of female gametophytes, pistils were isolated from WT and *atsec24bc* (+/*24b*, +/*24c*) flowers at floral stage 14. The pistils were fixed, dehydrated, and cleared as previously described [11]. The ovules were enclosed in immersion oil with a coverslip and observed using a TCS SP5 CLSM (Leica Microsystems) equipped with a HCX PL APO CS 63.0x1.40 OIL UV objective

lens. The ovules were illuminated with an argon laser (488 nm) and autofluorescence was viewed at a wavelength of 500-600 nm.

Table 2-1 Oligonucleotides used in this study

Oligos	Sequence
AtSec24A-att B1	5'-AAAAAGCAGGCTCCGACACTATGGGTACGGAGAATCAGGG-3'
AtSec24A-att B2	5'-AGAAAGCTGGGTAGACACTGTTTTGTTGAACTTGGCGGTGAAG-3'
AtSec24B-att B1	5'-AAAAAGCAGGCTCCGACACTATGGCTGCTCCAGTGCCTCC-3'
AtSec24B-att B2	5'-AGAAAGCTGGGTAGACACTGTTCAGTTTGTGTTGGATTTGAC-3'
AtSec24C-att B1	5'-AAAAAGCAGGCTCCGACACTATGGTTGCTCCTGTGCCTCC-3'
AtSec24C-att B2	5'-AGAAAGCTGGGTAGACACTGTTCATTTTTAGCTGGATTTGG-3'
SYP31-att B1	5'-AAAAAGCAGGCTCCGACACTATGGGCTCGACGTTCAGAG-3'
SYP31-att B2	5'-AGAAAGCTGGGTAGACACTAGCCACAAAGAAGAGGAAAA-3'
AtSec24A-pro-att B1	5'-AAAAAGCAGGCTCCGACACTCATACGCTTACGGAGAAACCTCATG-3'
AtSec24A-pro-att B2	5'-AGAAAGCTGGGTAGACACTTATTGATCACAACTTATCACTTACAACAGTTG-3'
AtSec24B-pro-att B1	5'-AAAAAGCAGGCTCCGACACTGACAAGGATGACTGAATGAG-3'
AtSec24B-pro-att B1r	5'-TGTACAAACTTGTGACACTGCTTGTTTACCAAAGAGATC-3'
AtSec24B-pro-att B2	5'-AGAAAGCTGGGTAGACACTGCTTGTTTACCAAAGAGATC-3'
AtSec24C-pro-att B1	5'-AAAAAGCAGGCTCCGACACTGCGCTTCCTGAGGTAACGAACC-3'
AtSec24C-pro-att B2	5'-AGAAAGCTGGGTAGACACTGCTTGGATACGAGATGGAGATCAAATC-3'
AtSec24B-pro-att B4	5'-GAAAAGTTGGCTGAGACACTGACAAGGATGACTGAATGAG-3'
AtSec24B-pro-att B1	5'-TGTACAAACTTGTGACACTGCTTGTTTACCAAAGAGATC-3'
AtSec24A-F	5'-GTCCGCAAAATTGGATGATG-3'
AtSec24A-R	5'-GTTTTGTTGAACTTGGCGGTGAAG-3'
AtSec24B-F	5'-CAGAGGATCACAATTCACAA-3'
AtSec24B-R	5'-CTCTCACCAAAGTCCACAAC-3'
AtSec24C-F	5'-TCCTTCAGCACCTTACGCT-3'
AtSec24C-R	5'-AACTTCATGAAAGGATTTAT-3'
ACT2-F	5'-CATCTTCTTCCGCTCTTTCTTTCCA-3'
ACT2-R	5'-CTCTTACAATTTCCCGCTCTGCTGT-3'
AtSec24C-PCRd-F	5'-CTGCCATGGGCCAACCTGGT-3'
AtSec24C-PCRd-R	5'-CTCAGATAGCTGAACTACA-3'
atsec24b-R	5'-AACATAGGTTCATGTCAGCA-3'
atsec24c-F	5'-CTCATTGTATTCCTTGATTC-3'
atsec24c-R	5'-GTATCGCATTCATTGAGACA-3'
T-DNA-LB	5'-GCAATCAGCTGTTGCCCGTCTCACTGGAG-3'

Results

A. thaliana Sec24 homologs, *AtSec24B* and *AtSec24C* are highly homologous

The Arabidopsis genome possesses multiple homologs of each COPII components. There are five Sar1, two Sec13, two Sec31, seven Sec23, and three Sec24 homologs [46]. The three Sec24 homologs in *A. thaliana* are AtSec24A (At3g07100), AtSec24B (At3g44340), and AtSec24C (At4g32640) [36-38]. A phylogenic tree of Sec24 orthologs of budding yeast, animals, and plants shows that the Sec24 family is comprised of five subgroups. These subgroups separate AtSec24B and AtSec24C into one group and AtSec24A into another (Figure 2-1a). AtSec24A, an Arabidopsis Sec24 isoform, localizes in

the cytoplasm and ERES in plant cells [30,32,35]. AtSec24B is an equivalent of *clone eighty-four* conferring tolerance to oxidative stress in budding yeast [47]. AtSec24C, which is highly homologous to AtSec24B, has not been characterized.

Because exact CDSs for *AtSec24B* and *AtSec24C* have not been experimentally confirmed, the author isolated and sequenced full-length cDNAs for *AtSec24B* and *AtSec24C* that were synthesized from WT mRNA. The cDNA sequence for *AtSec24B* was 3291 bp, and was identical to that listed in the *A. thaliana* database (TAIR: http://www.arabidopsis.org). However, the determined CDS of *AtSec24C* (3279 bp) was 36 bp longer than the predicted CDS shown in the database. The additional 36 bp correspond 3′ region of the sixteenth intron of the sequence in the TAIR database and the deduced 12 amino acids are located in the β-barrel domain of the AtSec24C protein as shown in Figure 2-2. The revised amino acid sequence of *AtSec24C* is 1092 amino acids and has 76% identity to that of *AtSec24B*. The CDS sequence of AtSec24C can be found in the GenBank/EMBL/DDBJ database under accession nos. AB778564.

The yeast Sec24 polypeptide (ScSec24p) is folded into five distinct domains: a β-barrel, a zinc finger, a ‘trunk’ domain, an all-helical region and a gelsolin-like domain [7]. All these domains are highly conserved in AtSec24A, AtSec24B, and AtSec24C, but AtSec24s had longer N-terminal extensions than ScSec24p (Figure 2-1b). As reported previously [36], the amino acid residues that contribute to the binding of cargo in budding yeast also exist in AtSec24A, AtSec24B, and AtSec24C (Figure 2-2). These results suggest that AtSec24B and AtSec24C, in addition to AtSec24A, are involved in sorting of cargo destined for incorporation into COPII vesicles in *A. thaliana*.

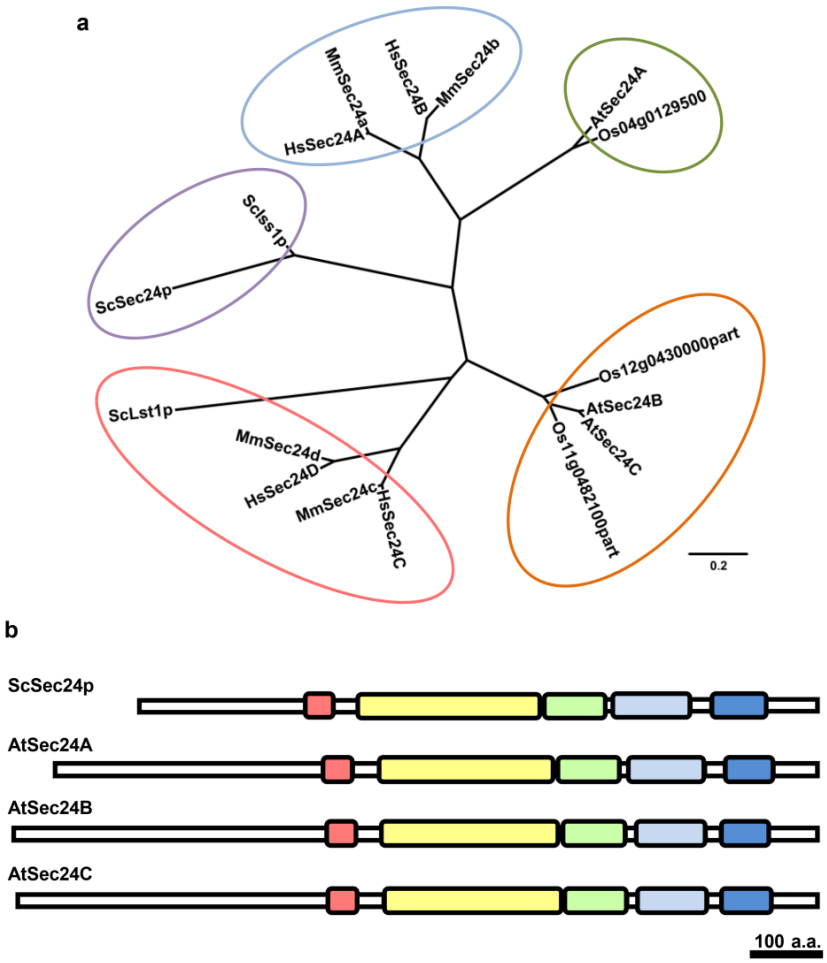

Fig. 2-1 Comparison of the protein sequence and structure of Sec24 orthologs in different organisms

a A phylogenetic tree of the Sec24 family including Sec24 family members from *Arabidopsis thaliana*, *Oryza sativa*, *Homo sapiens*, *Mus musculus*, and *Saccharomyces cerevisiae*. In accordance with multiple alignment of peptide sequences, the phylogenetic tree was created using ClustalW version 1.83 (http://clustalw.ddbj.nig.ac.jp/) with neighbor-joining method and bootstrap analysis (1,000 replication) and was drawn using GENETYX-Tree (Genetyx, Tokyo, Japan). Accession nos.: AtSec24A (*A. thaliana*, NP_187366), AtSec24B (*A. thaliana*, NP_566869), AtSec24C (*A. thaliana*, BAM76809), Os04g0129500 (*O. sativa*, NP_001052091), Os11g0482100part (*O. sativa*, NP_001067901), Os12g0430000part (*O. sativa*, NP_001066677), HsSec24A (*H. sapiens*, NP_068817), HsSec24B (*H. sapiens*, NP_006314) HsSec24C (*H. sapiens*, NP_940999), HsSec24D (*H. sapiens*, NP_055637), MmSec24a (*M. musculus*, NP_780464) MmSec24b (*M. musculus*, NP_997092), MmSec24c (*M. musculus*, NP_766184), MmSec24d (*M. musculus*, NP_081411), ScSec24p (*S. cerevisiae*, AAT92907), ScIss1p (*S. cerevisiae*, AAT92847), and ScLst1p (*S. cerevisiae*, NP_011966). The scale bar indicates an evolutionary distance. **b** Schematic diagram of structures of ScSec24p and Sec24 homologs in *A. thaliana*. The five domains were identified using the the Pfam protein families database (http://pfam.sanger.ac.uk/): zinc finger domain (red), 'trunk' domain (yellow),β-barrel domain (green), all-helical region (light blue), and gelsolin-like domain (blue)

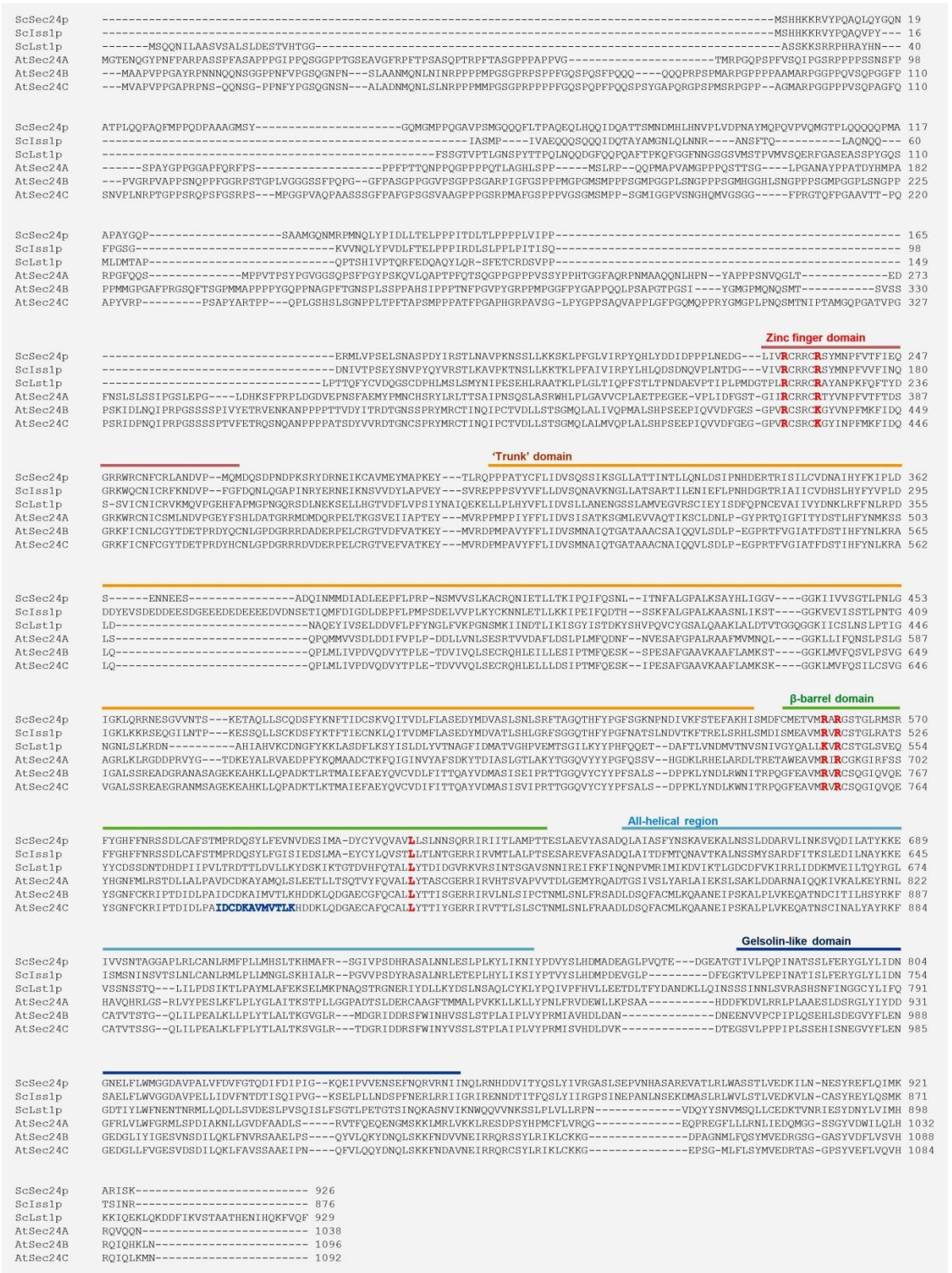
Zinc finger domain
'Trunk' domain
β-barrel domain
All-helical region
Gelsolin-like domain

Fig. 2-2 Multiple alignment of the amino acid sequences of ScSec24p, ScIss1p, ScLst1p, AtSec24A, AtSec24B, and AtSec24C

The amino acid sequences including Sec24 family members from *A. thaliana* and *S. cerevisiae* were aligned using the ClustalW version 1.83. Accession nos.: AtSec24A (*A. thaliana*, NP_187366), AtSec24B (*A. thaliana*, NP_566869), AtSec24C (*A. thaliana*, BAM76809), ScSec24p (*S. cerevisiae*, YIL109C), ScIss1p (*S. cerevisiae*, YNL049C), and ScLst1p (*S. cerevisiae*, YHR098C). To find the sequences corresponding to the five domains, the ScSec24p amino acid sequence and the motif database Pfam were used: zinc finger domain (rose), 'trunk' domain (yellow),β-barrel domain (green), all-helical region (light blue), and gelsolin-like domain (blue). The red letters indicate the essential amino acid residues for binding of cargo in budding yeast Sec24 family members reported by Miller *et al.* (2003). These amino acid residues are conserved in AtSec24s. The blue letters indicate the newly added 12 amino acids of AtSec24C determined in this study

AtSec24s are expressed in most organs of *A. thaliana*

To investigate the expression pattern of the *AtSec24* genes, the author performed RT-PCR analysis using mRNAs isolated from four major tissues: root, true leaf, stem, and inflorescence. *AtSec24A* was detected in all tissues at the same level (Figure 2-3a). By contrast, expression of *AtSec24B* and *AtSec24C* showed preferential expression; expression in the root and inflorescence was higher than that in the true leaf and stem (Figure 2-3a). To analyze the expression pattern of these genes in detail, the author performed promoter:GUS assays. The GUS staining of *AtSec24A*, *AtSec24B*, and *AtSec24C promoter:GUS* transgenic lines was essentially the same during the seedling stage (5-15 days after germination). The GUS activity expressed under the *AtSec24A* promoter was detected throughout the whole seedling and localized in the vascular bundle of the young seedlings at 5 days after germination (Figure 2-3b). The GUS activities from the *AtSec24B* and *AtSec24C* constructs were observed in the same region as that from the *AtSec24A* construct (Figure 2-3h and n). In 15-days-old seedlings, the GUS activity from *AtSec24A* was observed throughout the whole body (Figure 2-3c). High levels of GUS activity were detected in the roots and veins of cotyledons and true leaves. The GUS staining from *AtSec24B* and *AtSec24C* constructs showed the same pattern as that of *AtSec24A* (Figure 2-3i and o). A higher level of expression was detected at root tips and in the veins of cotyledons and true leaves in *AtSec24B promoter:GUS* transgenic plants (Figure 2-3i), and in the

root and the veins of cotyledons and true leaves in *AtSec24C promoter:GUS* transgenic plants (Figure 2-3o).

For flowers and siliques, the GUS staining of *AtSec24A* transgenic plants was observed in the ovules, pollen grains (Figure 2-3d and e), and embryos (Figure 2-3f). The GUS activity in the embryos became weaker as the silique developed (Figure 2-3f and g). The GUS activity from the *AtSec24B* construct was detected in sepals, petals, stamens with pollen grains, pistils, and flower buds (Figure 2-3j and k). The ovary was strongly stained at a young stage. The GUS staining in the pistil became weaker as it matured into a silique (Figure 2-3j, l, and m). The GUS activity from the *AtSec24C* construct was observed in the sepals, stamens with pollen grains, pistils, and flower buds (Figure 2-3p and q). In siliques of *AtSec24C* transgenic plants, the GUS activity was detected in carpels, placenta, and suspensors (Figure 2-3r and s).

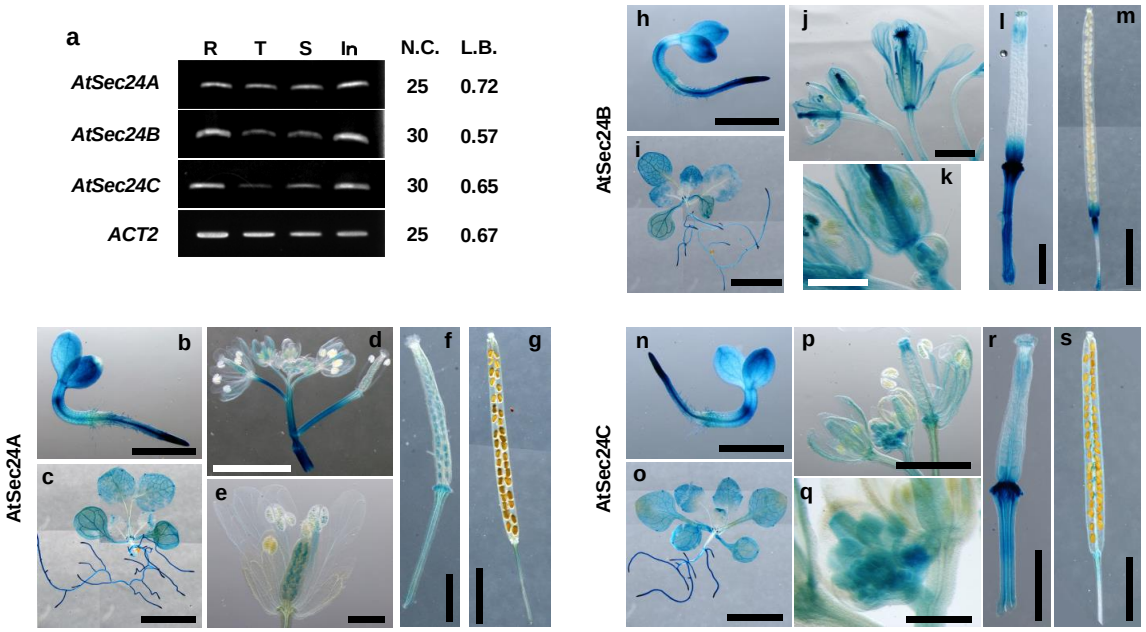

Fig. 2-3 Expression patterns of Sec24 homologs in *A. thaliana*
a RT-PCR analysis of *AtSec24s* expression using total RNA from roots (R), true leaves (T), stems (S) and inflorescences (In) from WT plants. *Actin2* transcript (*ACT2*) was amplified as a control. N.C.: the number of PCR cycles. L.B.: the length of detected bands (kbp). **b-g** GUS staining patterns of *AtSec24A promoter:GUS* transgenic plants: a young seedling (**b**), a seedling (**c**), an inflorescence (**d**), a flower (**e**), a young silique (**f**), and a silique (**g**). **h-m** GUS staining patterns of *AtSec24B promoter:GUS* transgenic plants: a young seedling (**h**), a seedling (**i**), an inflorescence (**j**), a young flower (**k**), a young silique (**l**), and a silique (**m**). **n-s** GUS staining patterns of *AtSec24C promoter:GUS* transgenic plants: a young seedling (**n**), a seedling (**o**), an inflorescence (**p**), a young flower (**q**), a young silique (**r**), and a silique (**s**). Scale bars = 1 cm (**b**, **f**, **h**, **j**, **l**, **n**, **p**, and **r**), 5 cm (**c**, **i**, and **o**), 3 cm (**d**, **g**, **m**, and **s**), 0.5 cm (**e** and **k**), and 0.3 cm (**q**)

AtSec24B and AtSec24C show subcellular distributions that are characteristic of COPII components in *A. thaliana*

In plant cells, AtSec24A fused with YFP at the N-terminus (YFP-AtSec24) localized in the cytoplasm and in punctate structures adjoined to a Golgi marker, which indicate the ERES [32]. The intracellular localization of AtSec24B and AtSec24C has not been experimentally examined, although they are predicted to have the N-terminal extension containing the targeting sequence for transport into chloroplasts by *in silico* analysis [34]. To determine the intracellular localization of AtSec24B and AtSec24C, the author fused GFP onto the C-terminus of AtSec24s to avoid interference with the chloroplast-targeting function of the N-terminal region, and observed the GFP-fused AtSec24s by CLSM. These constructs were transiently expressed in *A. thaliana* leaf epidermal cells by particle bombardment. AtSec24B-GFP and AtSec24C-GFP were detected primarily in the cytoplasm with bright punctate structures that are judged to be ERES from their similarity to punctate structure labeled with YFP-AtSec24 shown in a previous report [30,32] (Figure 2-4a and b). Consistent with previous reports on YFP-AtSec24A, the fluorescence of AtSec24A-GFP was observed primarily in the cytoplasm with bright punctate structures (Figure 2-4c).

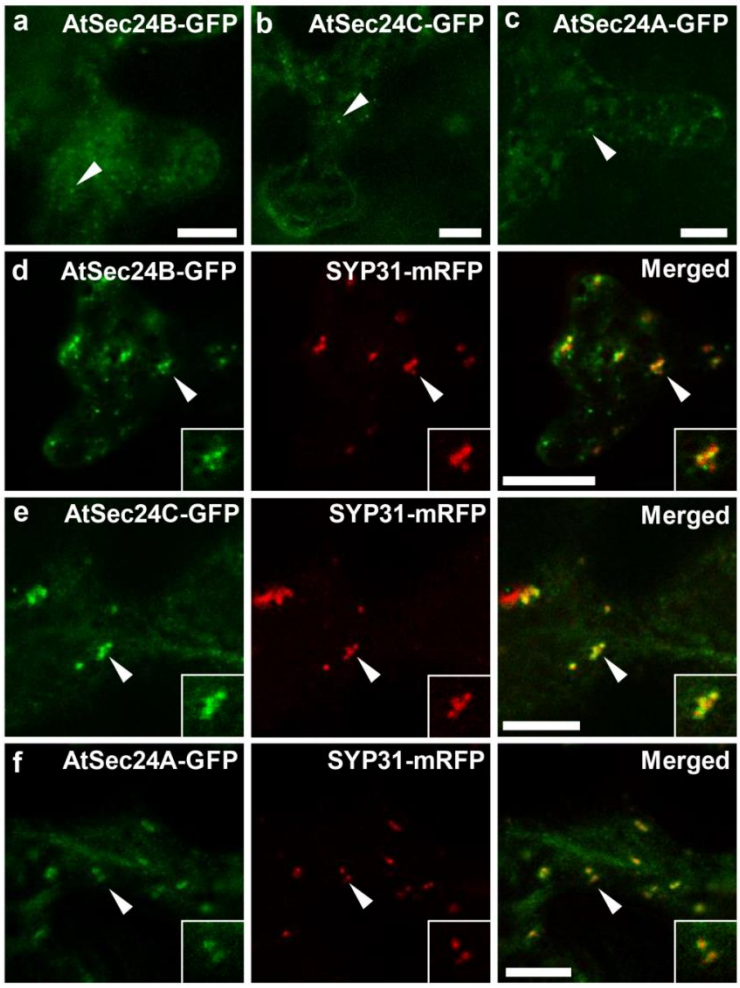

Fig. 2-4 Intracellular distribution of Sec24 homologs in *A. thaliana*
a-c Distributions of AtSec24B-GFP (**a**), AtSec24C-GFP (**b**), and AtSec24A-GFP (**c**) in *A. thaliana* leaf epidermal cells. Arrowheads indicate bright punctate structures labeled with GFP. **d-f** Localization of AtSec24B-GFP (**d**), AtSec24C-GFP (**e**), and AtSec24A-GFP (**f**) when co-expressed with SYP31-mRFP in Arabidopsis leaf epidermal cells. Left and middle panels show GFP (green) and RFP fluorescence (red), respectively, and are merged in right panels. Insets show magnified images of the adjacent GFP-labeled punctate structures and the RFP-labeled Golgi indicated by arrowheads. Scale bars = 10 μm

To confirm that the punctate structures labeled with GFP were ERES, the author co-expressed AtSec24s-GFP with a Golgi marker fused to mRFP. The Qa-syntaxin SYP31 is an *A. thaliana* homolog of yeast Sed5p, which binds Sec24p in yeast [48,49], and is transported to the Golgi through the secretory pathway [50]. Because C-terminally-tagged fluorescent SYP31 localize to Golgi body without interrupting ER-to-Golgi traffic [50,51], the author constructed C-terminal mRFP-tagged SYP31 (SYP31-mRFP) and tested

whether it localized to the Golgi by co-expression with well-known Golgi marker ST-GFP (GFP fused to the 52 N-terminal amino acids of rat 2,6-sialyl transferase) [52]. SYP31-mRFP colocalized with ST-GFP (Figure 2-5), which suggests that SYP31-mRFP was localized at the Golgi body in leaf epidermal cells. When SYP31-mRFP was co-expressed with AtSec24B-GFP (Figure 2-4d) or AtSec24C-GFP (Figure 2-4e), GFP fluorescence was detected in the cytoplasm and at prominent bright punctate structures. In addition, these dots of GFP fluorescence were adjoined by RFP dots and moved around the cytoplasm (data not shown). The same localization pattern was obtained when AtSec24A-GFP and SYP31-mRFP were co-expressed (Figure 2-4f), and the fluorescence images of all AtSec24s-GFP were similar to those published in a previous report [32]. These results show that AtSec24A, AtSec24B, and AtSec24C are diffusely distributed in the cytoplasm under normal conditions. Recruitment of AtSec24s to ERES is facilitated by overexpression of a cargo SYP31, which indicates that AtSec24s contributes to COPII formation. In this experiments, plastid localization of AtSec24B and AtSec24C was not observed (Figure 2-6); this result disagrees with that of an *in silico* localization analysis [34].

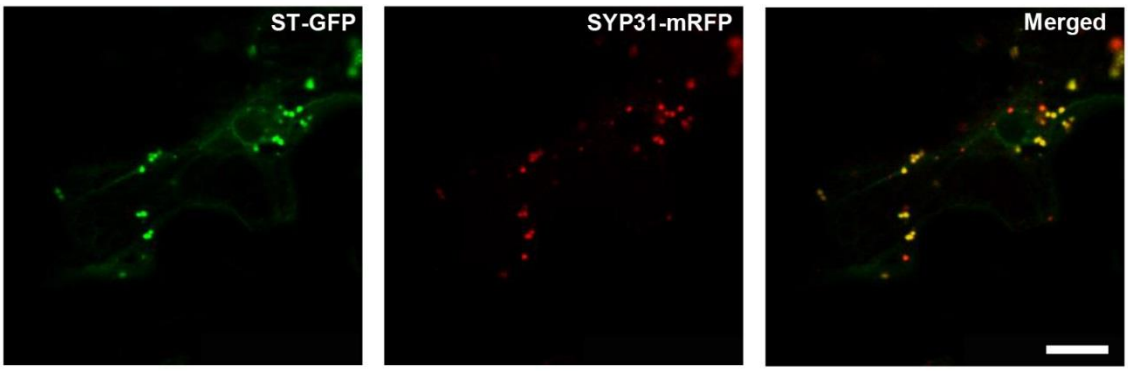

Fig. 2-5 Colocalization of SYP31-mRFP and ST-GFP in *A. thaliana* epidermal cells
Confocal images of *A. thaliana* leaf epidermal cells co-expressing SYP31-mRFP and the Golgi marker ST-GFP. ST-GFP (*P_{35S}:ST-GFP*) and pUGW54-*SYP31* plasmids were mixed at ratio of 1:1 and introduced into leaf epidermal cells of wild-type plants by the method described in the experimental procedures. The left and middle panels show GFP (green) and RFP fluorescence (red), respectively, and are merged in the right panel. Golgi apparatus labeled by ST-GFP colocalized with the structures labeled by SYP31-mRFP, as indicated by yellow punctate structures in the merged image. The sale bar = 10 μm

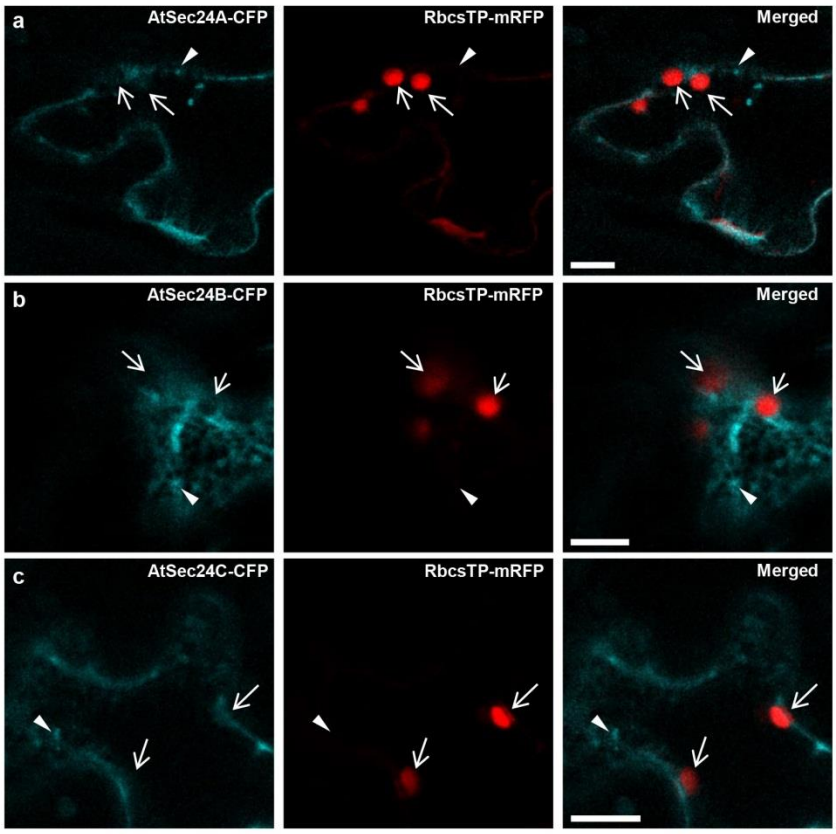

Fig. 2-6 Subcellular localization of Arabidopsis Sec24 homologs co-expressed with chloroplast marker in *A. thaliana* leaf epidermal cells

Confocal images of *A. thaliana* leaf epidermal cells co-expressing cyan fluorescent protein (CFP) fused AtSec24s and the chloroplast marker. For transient expression of mRFP linked to chloroplast transit peptide of ribulose 1,5-bisphosphate carboxylase/oxylase small subunit (RBCS) 1A under control of P_{35S} as a chloroplast marker, pRbcsTP221 donated by Dr. Shoji Mano (National Institute for Basic Biology) was introduced into pUGW54 [36] by LR reaction, which generated pUGW54-*RbcsTP*. To generate clones for expressing AtSec24s fused CFP under control of P_{35S} (pUGW44-*AtSec24s*), pDONR201-*AtSec24s* entry clones were introduced into pUGW44 [36] by the LR reaction. pUGW44-*AtSec24s* and pUGW54-*RbcsTP* plasmids were mixed at ratio of 8:1 and introduced into leaf epidermal cells of wild-type plants by the method described in the experimental procedures. The cells were viewed with a TCS SP5 CLSM (Leica Microsystems) using an HCX PL APO CS 63.0x1.20 WATER UV objective lens. The CFP was exited with the argon laser line (458 nm) and the CFP fluorescence was detected at 465-510 nm. The RFP fluorescence was obtained under same condition described in the experimental procedures. Images were processed with Photoshop CS6 (Adobe Systems). The left and middle panels show CFP (cyan) and RFP fluorescence (red), respectively, and are merged in the right panel. Arrowheads and arrows indicate punctate structures and plastids in Arabidopsis leaf epidermal cells, respectively. As in case of AtSec24s-GFP, CFP fused AtSec24s were localized in the cytoplasm with bright punctate structures. AtSec24B-CFP (**b**) and AtSec24C-CFP (**c**), as well as AtSec24A-CFP (**a**), did not show the subcellular localization pattern as plastids labeled by RbcsTP-mRFP. Sale bars = 10 µm

A lack of AtSec24B impairs pollen germination activity

To investigate the functions of AtSec24B and AtSec24C in *A. thaliana*, the author used two T-DNA insertion lines; *atsec24b-1* (SALK_013076) carries an insertion in the first intron of *AtSec24B*, and *atsec24c-1* (SALK_001648) contains an insertion in the fifth intron of *AtSec24C* (Figure 2-7). RT-PCR analysis showed defect of the corresponding transcript in *atsec24b-1* plant, whereas a few amount of *AtSec24C* transcript was detected in *atsec24c-1* plant (Figure 2-7). Next, the author examined segregation in self-fertilized progeny of heterozygous *atsec24b-1* (+/*24b*) and *atsec24c-1* (+/*24c*). The segregation ratio of self-fertilized progeny of heterozygous *atsec24c-1* (+/*24c*) was approximately 1 (+/+): 2 (+/*24c*): 1 (*24c*/*24c*), which shows good agreement with Mendel's law. However, in self-fertilized progeny of heterozygous *atsec24b-1* (+/*24b*), the segregation rate of homozygous *atsec24b-1* (*24b*/*24b*) was 13%, which is less than the expected value from Mendel's law (Table 2-2). This result indicates that the penetration of the *atsec24b-1* allele into offspring was impaired. To evaluate gametophyte specificity for transmission of the *atsec24b-1* allele, the author performed reciprocal crosses of heterozygous *atsec24b-1* (+/*24b*) with WT (+/+). In crosses between the *atsec24b-1* (+/*24b*) female parent and the WT male parent, the appearance of heterozygous F_1 progeny (+/*24b*) was 52% (Table 2-2). However, in crosses between *atsec24b-1* (+/*24b*) male parent and WT female parent, the appearance of heterozygous F_1 progeny (+/*24b*) was 29% (Table 2-2), which is less than the value expected from Mendel's law. These results suggest that the transmission of the *atsec24b-1* allele was normal via female gametophyte but impaired via male gametophyte. In the reciprocal cross between *atsec24c-1* (+/*24c*) and WT (+/+), irrespective of which parents from *atsec24c-1* (+/*24c*) were crossed with the WT parental partner, the segregation ratio was almost 1 (+/+): 1 (+/*24c*) (Table 2-2).

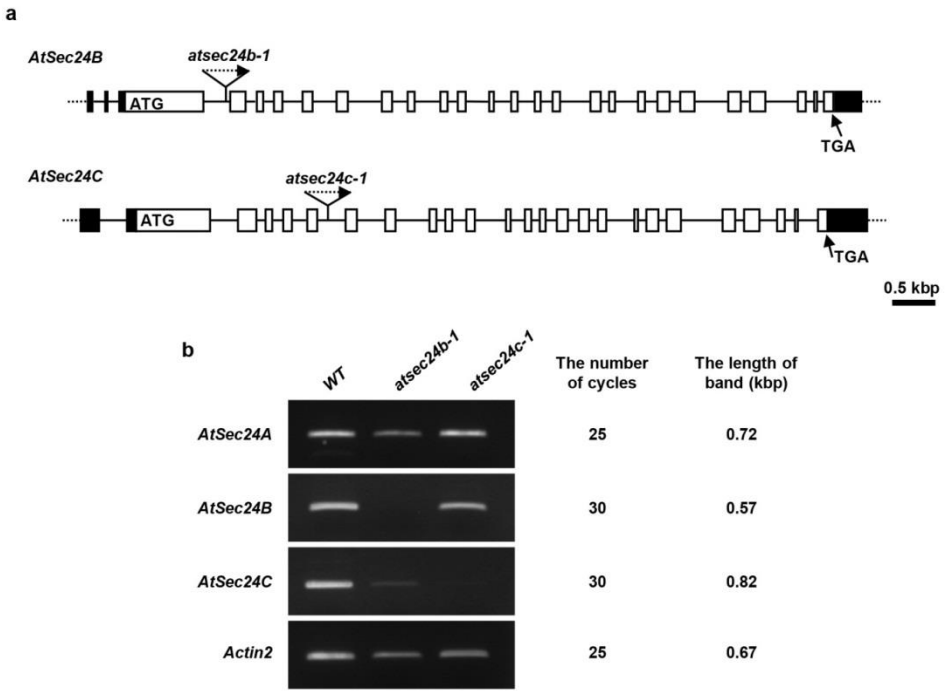

Fig. 2-7 Schematic diagram of genomic *AtSec24B* and *AtSec24C* genes and RT-PCR analysis in *atsec24b-1* and *atsec24c-1* plants

a Schematic diagram of T-DNA insertion sites in genomic *AtSec24B* and *AtSec24C* genes. The white and black boxes indicate exons and untranslated regions, respectively. The solid lines show introns. ATG and TGA indicate initiation codons and termination codons in *AtSec24B* and *AtSec24C*, respectively. The arrows with a broken line indicate T-DNA and the direction it is inserted in each *AtSec24* gene. **b** RT-PCR analysis using *atsec24b-1* and *atsec24c-1* plants. Total RNAs were isolated from WT and each mutant grown on Jiffy-7 (Jiffy Preforma Production K.K). cDNAs were synthesized with an oligo-dT primer using ReverTraAce (TOYOBO). To amplify *AtSec24A*, *AtSec24B*, and *Actin2*, PCR was performed using the conditions described in the experimental procedures. To specifically detect disruption of *AtSec24C*, PCR was performed with 30 cycles using cDNA isolated from each plant as a template and the *AtSec24C-PCRd*-F and *AtSec24C-PCRd*-R primers (Table 2-1)

Table 2-2 Segregation of *atsec24b-1* and *atsec24c-1* alleles in various crosses

Parental genotype		Total (*n*)	Genotype of progeny		
Male	Female		+/+* (%)	+/*t** (%)	*t*/*t** (%)
+/*24b*	+/*24b*	126	48	39	13
+/*24b*	+/+	65	71	29	0
+/+	+/*24b*	67	48	52	0
+/*24c*	+/*24c*	129	25	51	24
+/*24c*	+/+	68	53	47	0
+/+	+/*24c*	63	49	51	0

*+/+ indicate wild type and +/*t* and *t*/*t* indicate heterozygote and homozygote for the T-DNA inserted mutants, respectively

The male gametophytes (pollen) develop in the anther and are released after maturation. Released pollen germinates on stigma and grows pollen tube toward the ovule to transfer sperm cells to female gametophytes. First, to examine the developmental defect of pollen possessing the *atsec24b-1* allele, DAPI staining and Alexander staining [53] were performed. All mature pollen from *atsec24b-1* (*24b*/*24b*) plants were stained red-purple by Alexander stain (Figure 2-8a), which suggests that pollen carrying the *atsec24b-1* allele were viable. DAPI staining revealed that most mature pollen carrying the *atsec24b-1* allele possessed three nuclei (two sperm nuclei and one vegetative nucleus), which was also observed in WT pollen (Figure 2-8b). These results indicate that the mature pollen developed normally. Second, to test whether pollen defective in AtSec24B can germinate, the author performed an *in vitro* pollen germination assay as previously described [44]. In this assay, 84% of WT pollen germinated, whereas the germination rate of pollen from *atsec24b-1* (*24b*/*24b*) plants was reduced to 36% (Figure 2-8c). This germination defect was restored by expression of AtSec24B-GFP under the native *AtSec24B* promoter in *atsec24b-1* (*24b*/*24b*) plants (Figure 2-8c). These results indicate that pollen defective in AtSec24B developed and matured normally but were impaired in germination, which caused a reduction in pollen fertility.

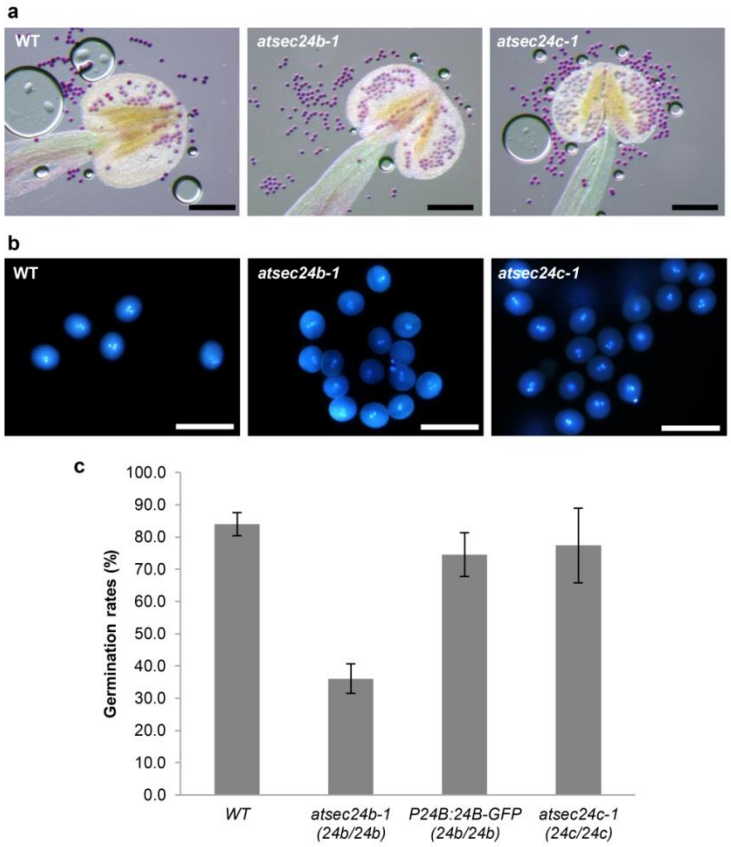

Fig. 2-8 Effect of AtSec24B knockout in male gametophytes
a Alexander staining of WT, homozygous *atsec24b-1*, and homozygous *atsec24c-1* plants. Scale bars = 0.2 mm. **b** DAPI staining of WT, homozygous *atsec24b-1*, and homozygous *atsec24c-1* plants. Scale bars = 50 µm. **c** Pollen germination rate of WT, homozygous *atsec24b-1* [*atsec24b-1* (*24b*/*24b*)], *atsec24b-1* complemented by *AtSec24B promoter:AtSec24B-GFP* [*P24B:24B-GFP* (*24b*/*24b*)] and homozygous *atsec24c-1* [*atsec24c-1* (*24c*/*24c*)] plants. Bars show means of at least three independent tests. Error bars = ± SD

Coexistence of *atsec24b-1* and *atsec24c-1* alleles is associated with defective gene transmission via gametophytes

Next, the author performed crosses between *atsec24b-1* (*24b*/*24b*) and *atsec24c-1* (*24c*/*24c*) plants and checked the genotype of F_2 progenies to isolate double homozygous *atsec24bc* (*24b*/*24b*, *24c*/*24c*). Because *AtSec24B* and *AtSec24C* are located on different chromosomes (At3g44340 and At4g32640, respectively), the theoretical segregation rate of F_2 from self-fertilized F_1 (+/*24b*, +/*24c*) is 1 (+/+, +/+): 2 (+/+, +/*24c*): 1 (+/+, *24c*/*24c*):

2 (+/*24b*, +/+): 4 (+/*24b*, +/*24c*): 2 (+/*24b*, *24c*/*24c*): 1 (*24b*/*24b*, +/+): 2 (*24b*/*24b*, +/*24c*): 1 (*24b*/*24b*, *24c*/*24c*). The genotyping result is summarized in Table 2-3. F_2 plants expressing the genotypes (+/*24b*, *24c*/*24c*), (*24b*/*24b*, +/*24c*), and (*24b*/*24b*, *24c*/*24c*) were not found in a total of 104 F_2 progenies investigated (Table 2-3). These results suggest that the co-transmission of *atsec24b-1* and *atsec24c-1* alleles is impaired through gametophytes. To investigate the gametophyte specificity for the defect in co-transmission, the author performed the reciprocal cross of double heterozygous *atsec24bc* (+/*24b*, +/*24c*) with WT (+/+). If gametophytes possessing *atsec24b-1* and *atsec24c-1* alleles can develop normal fertility, the theoretical segregation rate of F_1 progeny is 1 (+/+, +/+): 1 (+/*24b*, +/+): 1 (+/+, +/*24c*): 1 (+/*24b*, +/*24c*) in this cross. The results are shown in Table 2-4. No F_1 plants of the genotype (+/*24b*, +/*24c*) were found in the cross of male gametophytes from *atsec24bc* (+/*24b*, +/*24c*), nor in the cross of female gametophytes from *atsec24bc* (+/*24b*, +/*24c*). These results suggest that the co-penetration of *atsec24b-1* and *atsec24c-1* alleles into offspring is prohibited via both male and female gametophytes.

Table 2-3 Inheritance pattern of *atsec24b-1* and *atsec24c-1* alleles in self-fertilization of *atsec24bc* (+/*24b*, +/*24c*) lines

F_1 genotype	Genotype of F_2 progeny* (*n*)								
	+/+, +/+	+/+, +/24c	+/+, 24c/24c	+/24b, +/+	+/24b, +/24c	+/24b, 24c/24c	24b/24b, +/+	24b/24b, +/24c	24b/24b, 24c/24c
+/24b, +/24c	22	29	9	22	15	0	7	0	0

*A total of 104 F_2 progenies from self-fertilized F_1 (+/*24b*, +/*24c*) were investigated in this assay

Table 2-4 Inheritance pattern of *atsec24b-1* and *atsec24c-1* alleles in reciprocal cross of *atsec24bc* (+/*24b*, +/*24c*) line with WT

Parental genotype		Genotype of back cross F_1 progeny (*n*)			
Male	Female	+/+, +/+	+/24b, +/+	+/+, +/24c	+/24b, +/24c
+/24b, +/24c	+/+, +/+	26	9	18	0
+/+, +/+	+/24b, +/24c	10	16	20	0

Coexistence of *atsec24b-1* and *atsec24c-1* alleles affects gametogenesis

The cross between the male gametophyte from *atsec24bc* (+/*24b*, +/*24c*) and the female WT gametophyte showed that the male gametophyte was sterile under condition of reduced expression of *AtSec24B* and *AtSec24C*. To determine the mechanism of the male sterility, the author observed the pollen grains from *atsec24bc* (+/*24b*, +/*24c*) by SEM, because pollen grains aborted during development often have an abnormal shape [54,55]. For precise analysis, the author prepared *atsec24bc* (+/*24b*, +/*24c*) plants possessing homozygous *qrt1*-2 mutation [*atsec24bc* (+/*24b*, +/*24c*, *qrt1-2*/*qrt1-2*)]. Because pollen grains are released as tetrads in the *qrt1* mutant [56], the segregation of *atsec24b-1* and *atsec24c-1* alleles in four pollens developed from a microsporocyte can be predicted. In the *qrt1-2* mutant (*qrt1-2*/*qrt1-2*), 91% of released pollen tetrads contained four normal pollen grains with the characteristic reticulate pattern of the pollen wall. By contrast, in *atsec24bc* (+/*24b*, +/*24c*, *qrt1-2*/*qrt1-2*) plants, only 15% of pollen tetrads were composed of the four normal pollen grains, and most (65%) of them included one shrunken pollen grain without the reticulate patterning (Figure 2-9a and b). In addition, 18% and 2% of all pollen tetrads contained two or one normal pollen grain(s), respectively (Figure 2-9b). These segregation results of the tetrad phenotype indicate that a reduction of both AtSec24B and AtSec24C leads to a reduction of pollen fertility caused by abortion during pollen development.

To determine the defective developmental stages of microspores carrying *atsec24b-1* and *atsec24c-1* alleles, the author performed DAPI staining of microspores at different developmental stages. Nascent microspores generated by microsporogenesis possess only one nucleus; thereafter, they undergo two cycles of pollen mitosis (pollen mitosis I and II) to develop into mature pollen containing three nuclei. DAPI staining of microspore tetrads allowed him to classify pollen development into four distinct stages: mononuclear, binuclear, PMII, and trinuclear (Figure 2-9c). Almost all microspore tetrads from the *qrt1-2* mutant consisted of four stained microspores in all developmental stages (Figure 2-9d). Most microspore tetrads from *atsec24bc* (+/*24b*, +/*24c*, *qrt1-2*/*qrt1-2*) plants consisted of four stained microspores in mononuclear and binuclear stages, whereas in PMII and tri-nuclear stages, the majority of microspore tetrads were composed of three stained and one unstained microspore (Figure 2-9e). For microspore tetrads composed of four stained

microspores from *atsec24bc* (+/*24b*, +/*24c*, *qrt1-2*/*qrt1-2*) at PMII stage, the author applied high-resolution imaging analysis with CLSM, and observed that a few of them had one abnormal microspore with two nuclei of a similar size (data not shown). These results indicate that significant decrease of AtSec24B and AtSec24C causes abortion of pollen development during the binuclear stage.

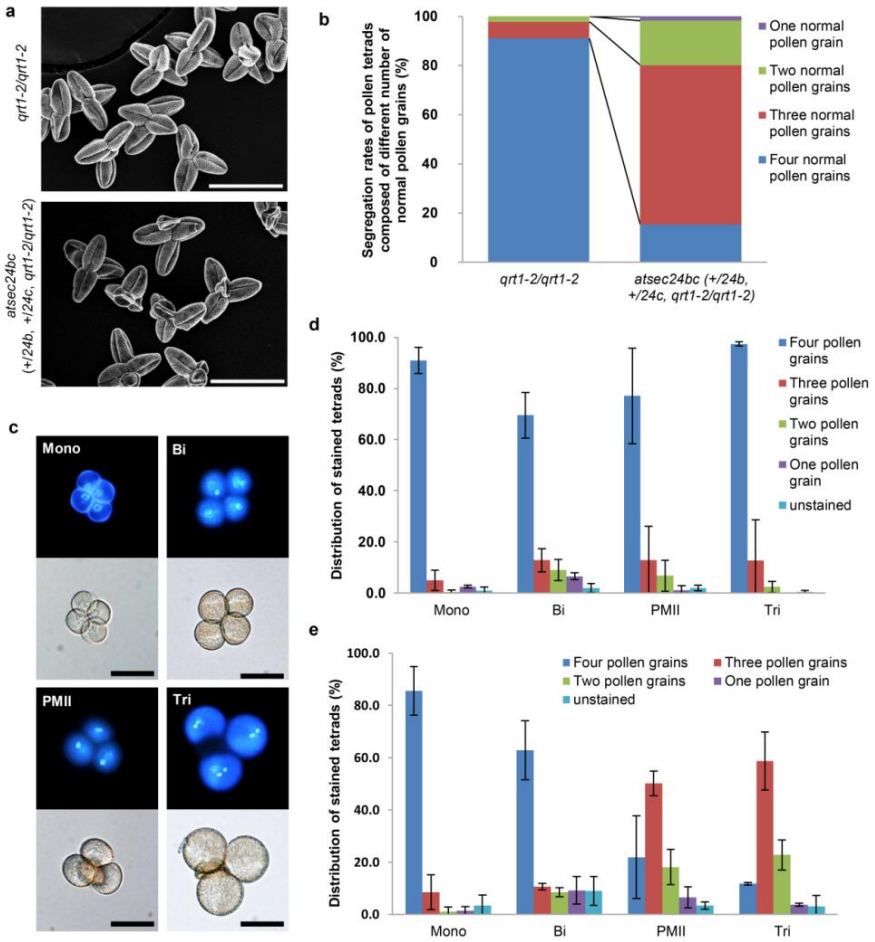

Fig. 2-9 Effect of decreased expression of AtSec24B and AtSec24C on male gametophytes

a SEM images of pollen tetrads isolated from *qrt1-2* (*qrt1-2*/*qrt1-2*) and *atsec24bc* (+/*24b*, +/*24c*) in *qrt1-2* background [*atsec24bc* (+/*24b*, +/*24c*, *qrt1-2*/*qrt1-2*)] plants. Scale bars = 50 µm. **b** Percentages of pollen tetrads with different numbers of normal pollen grains observed with SEM in *qrt1-2* and *atsec24bc* (+/*24b*, +/*24c*, *qrt1-2*/*qrt1-2*) plants. Colored bars show means of at least two independent observations. **c** DAPI fluorescence (upper panels) and bright-field images (lower panels) of pollen tetrads from *atsec24bc* (+/*24b*, +/*24c*, *qrt1-2*/*qrt1-2*) plants observed with a fluorescence microscope at developmental stages: mononuclear (Mono), binuclear (Bi), pollen mitosis II (PMII), and trinuclear (Tri). Scale bars = 20 µm. **d** and **e** Distribution of the number of DAPI-stained microspores in microspore tetrads from *qrt1-2* (**d**) and *atsec24bc* (+/*24b*, +/*24c*, *qrt1-2*/*qrt1-2*) plants (**e**) at each stage. Bars show means of at least two independent observations. Error bars = ± SD

To examine the influence on female gametogenesis by reduced expression of *AtSec24B* and *AtSec24C*, the author isolated ovules from pistils at floral stage 14 [57] and observed female gametophytes (embryo sacs) using CLSM according to previous reports [11,58]. The pistils in floral stage 14 contain mature embryo sacs that have a large central vacuole and a secondary endosperm nucleus produced by the fusion of two polar nuclei in the central cell [11]. In WT plants, 94% (n = 66) of ovules carried an embryo sac in agreement with the previous report. In *atsec24bc* (+/*24b*, +/*24c*) mutant plants, 72% (n = 110) of ovules possessed an embryo sac with the secondary endosperm nucleus and the central vacuole (Figure 2-10a) and some embryo sacs contained divided endosperm nuclei as a result of pollination. Nevertheless, 28% of mutant ovules exhibited various abnormalities in their embryo sacs (Figure 2-10b-e and 2-11). Approximately half of the mutant ovules contained embryo sacs arrested between two-nucleate to eight-nucleate stages (Figure 2-11). Furthermore, the majority of the embryo sacs displayed aberrant position and size of the central vacuole (Figure 2-10b and c). Three of the embryo sacs also contained an unusual number of nuclei (Figure 2-10d). The remaining half of abnormal ovules contained an autofluorescent structure, which was considered to be a degenerated megaspore (Figure 2-10e). These observations suggest that considerable decrease of both AtSec24B and AtSec24C disrupts serial mitosis in female gametogenesis and leads to defective formation of the central vacuole.

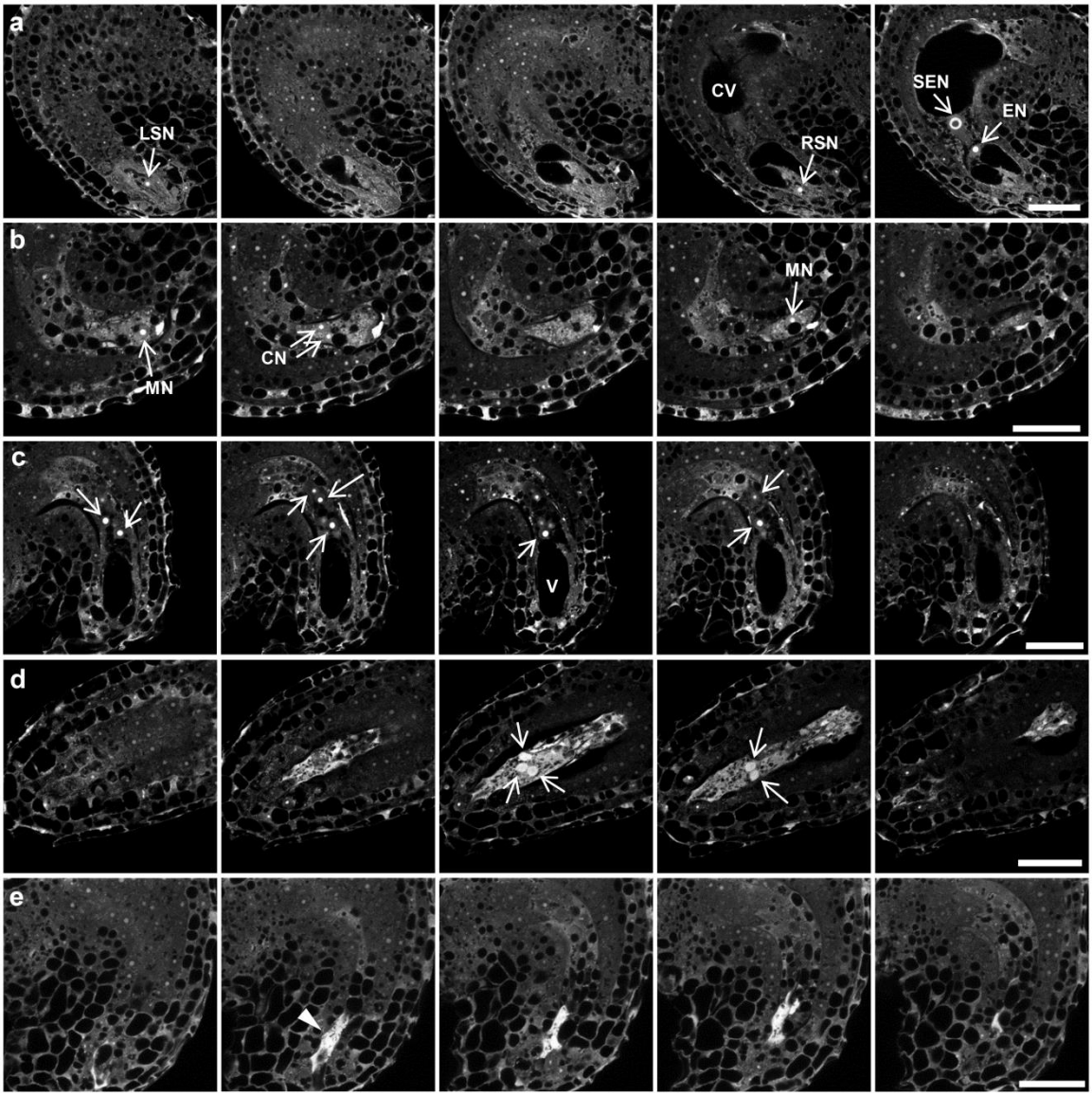

Fig. 2-10 Effect of decreased expression of *AtSec24B* and *AtSec24C* on female gametophytes

A series of CLSM images of distinct ovules isolated from *atsec24bc* (+/*24b*, +/*24c*) flowers at floral stage 14. Scale bars = 25 µm. **a** Ovule with a mature embryo sac containing a secondary endosperm nucleus and a central vacuole. **b** Ovule with an aberrant embryo sac containing four nuclei and small vacuoles. **c** Ovule with an aberrant embryo sac containing eight nuclei at the chalazal pole and a large vacuole at the micropylar pole. Arrows indicate the eight distinct nuclei. **d** Ovule with an embryo sac containing an abnormal number of nuclei. Arrows indicate the five distinct nuclei. **e** Ovule with an autofluorescent structure. Arrowhead indicates the autofluorescent structure. CN: chalazal nucleus, CV: central vacuole, EN: egg nucleus, LSN: left synergid cell nucleus, MN: micropylar nucleus, RSN: right synergid cell nucleus, SEN secondary endosperm nucleus, V: vacuole

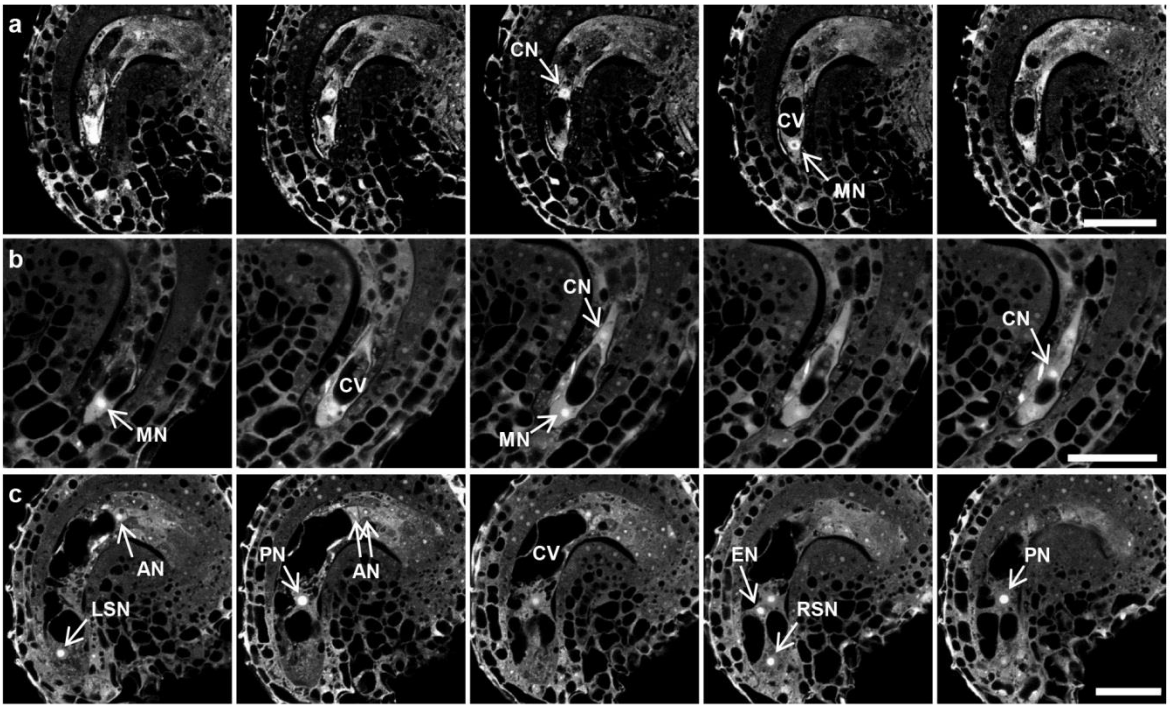

Fig. 2-11 A series of confocal images captured along the *z*-stack of ovules with an immature embryo sac in *atsec24bc* (+/*24b,* +/*24c*) flowers

All ovules were isolated from *atsec24bc* (+/*24b*, +/*24c*) flowers at floral stage 14. **a** Ovule containing an immature embryo sac arrested at the two-nucleate stage. **b** Ovule containing an immature embryo sac arrested at the four-nucleate stage. **c** Ovule containing an immature embryo sac with unfused polar nuclei. AN: antipodal cell nucleus, CN: chalazal nucleus, CV: central vacuole, EN: egg nucleus, LSN: left synergid cell nucleus, MN: micropylar nucleus, PN: polar nucleus, RSN: right synergid cell nucleus. Scale bars = 25 μm

Discussion

The formation of COPII vesicles, which mediate transport from the ER to the Golgi apparatus, is an important biological activity for eukaryotes. During the formation of COPII vesicles, Sec24 is thought to select the cargo proteins by direct binding [5,6]. It was known that Sec24 was conserved in fungi, mammal and plants [46,59]. Among three Sec24 homologs encoded in the *A. thaliana* genome, the subcellular dynamics and functions of AtSec24A are well characterized [30,32,35-38]. However, only sequence information was known for AtSec24B and AtSec24C, and their functional differences were unknown. In this study, the author analyzed the expression and intracellular localization of AtSec24A, AtSec24B, and AtSec24C, and did not find significant

differences among them. All three AtSec24s were expressed in most parts of the plant body and showed the same cytoplasmic localization patterns. However, the reverse genetic experiments using T-DNA inserted lines revealed the specific functions of AtSec24B and AtSec24C: a lack of AtSec24B leads to the reduction of pollen germination, and a significant reduction of both proteins caused defects in gametogenesis.

Throughout pollen development (with the exception of a period just after release of the microspore from the tetrad), the microspore appear to maintain a high level of secretory activity for the events described below [60-63]. In the tetrad after microsporogenesis, the microspores form primexine, which becomes the base of the outer pollen wall (exine), between the plasma membrane and the callose wall enveloping them. Microspores are released from the tetrad by decomposition of the callose form an intine consisting of cellulose and pectin between the plasma membrane and the exine. In microspores after pollen mitosis I, the generative cell and the vegetative cell are temporarily separated by the hemispherical cell wall including callose. After pollen mitosis II, the microspores are thought to begin to store materials required for pollen germination. The high-resolution imaging analysis showed that one microspore in the microspore tetrad had a generative nucleus whose chromatin is not condensed, suggesting that cytokinesis after pollen mitosis I did not occur in the microspore arrested at the binuclear stage. Like a cell plate formed during cytokinesis in plant somatic cells, callose wall formation is initiated by accumulation of Golgi-derived vesicles [64,65]. Because callose is not found in Golgi cisternae during cytokinesis of somatic cells and microsporocytes, callose synthase seems to be loaded into the Golgi vesicles [66,67]. CalS5, a callose synthase, is expressed throughout pollen development in *A. thaliana*, and is delivered to the phragmoplast by the secretory pathway in tobacco cultured cells [68,69]. Because AtSec24B-GFP and AtSec24C-GFP showed dynamic subcellular distributions characteristic of COPII components, AtSec24B and AtSec24C might be redundantly involved in the recognition of cargo that are required for the organization of the callose wall, such as CalS5. Pollen germination was reduced in homozygous *atsec24b-1* plants. The author found no remarkable abnormality in DAPI and Alexander staining in these plants; therefore, pollen of *atsec24b-1* plants likely have some defects that are undetectable by general cell staining analysis, a reduced supply of storage

proteins required for germination or defective secretion of a protein necessary to sense or respond to some signals for germination.

Loss of AtSec24A function induces defective transmission of the mutant allele via the male gametophyte, but not the female gametophyte, caused by reduction of pollen germination [39]. Compared to the results of the experiment using AtSec24B knockout plant, the degree of the defect in pollen germination differed between mutants with disrupted *AtSec24A* and *AtSec24B*. Therefore, AtSec24A and AtSec24B might play a partially different role in the transport of proteins required for cellular events involved in pollen development. Alternatively, because the microarray analysis of microspores indicated that the peak of *AtSec24A* expression appeared earlier than that of *AtSec24B* during development [39], this may also underlie the difference in the severity of the defects in pollen germination between the *AtSec24A* and *AtSec24B* mutants.

The female gametophyte of *A. thaliana* is a monosporic embryo sac undergoing *Polygonum*-type megagametogenesis [11]. A functional megaspore remains after meiosis and gives rise to karyokinesis to produce two nuclei. The two nuclei are separated into the chalazal and micropylar poles by a central vacuole. The two-nucleate embryo sac undergoes two rounds of karyokinesis to generate an eight-nucleate cell, and then produces a seven-celled female gametophyte after cellularization. After fusion of the two polar nuclei and degeneration of the antipodal cells, the seven-celled female gametophyte eventually develops into the four-celled mature embryo sac. The observations of embryo sacs from *atsec24bc* (+/*24b*, +/*24c*) plants suggest that the considerable decrease of AtSec24B and AtSec24C disrupts the progress of serial mitosis in megagametogenesis and causes abnormalities in the location and formation of nuclei and vacuoles. Many mutants defective in female gametophyte development have been isolated and characterized [58,70]. A SNARE protein, SEC22, contributes to membrane fusion in vesicle transport between the ER and Golgi, and is required for gametogenesis [71]. In a *sec22* mutant, microspores fail to enter pollen mitosis II, similar to the *atsec24bc* mutant, whereas the only defect of megaspores was in polar nuclei fusion in the central cell. SLOW WALKER (SWA) 1 and 2 are nucleolar proteins that are likely involved in ribosome biogenesis, and the loss of these protein induces delay of female gametophyte development at the two- to eight-nucleate stages [72,73], resembling the phenotypes of the *atsec24bc* mutant found in this study.

However, unlike the results in the *atsec24bc* mutant, no aberration of the vacuoles was reported in the papers describing the *swa1* and *2* mutants. Although the molecular mechanisms giving rise to abnormalities caused by reduced expression of *AtSec24B* and *AtSec24C* are unclear, this study might be a cue to understand the significance of secretory activity in megagametogenesis.

This study indicates not only AtSec24A but also AtSec24B and AtSec24C are involved in male gametogenesis and COPII transport mediated by AtSec24B and AtSec24C also play an important role in serial mitosis in female gametogenesis with formation of the central vacuole.

Chapter 3

Development of a pGWB series possessing a tunicamycin resistance gene as a marker for the transformation of *A. thaliana*

A large number of experimentally useful transgenic plants have been established: for example, T-DNA insertion mutant lines of *A. thaliana*, marker lines expressing a reporter gene in specific cells or tissues, and organelle marker lines making visible a specific organelle with a fluorescent protein [74]. The introduction of a transgene into these pre-existing transgenic lines is an important method in the functional analysis of the transgene [75] and the localization of its product. For example, in experiments of Chapter 2, the T-DNA inserted in *atsec24b-1* and *atsec24c-1* possesses a kanamycin resistance marker [76], and the binary vector (R4pGWB550) [15] used for expression of AtSec24B-GFP in *atsec24b-1* (*24b*/*24b*) plants carries hygromycin resistance marker. To complement the decrease of *AtSec24B* and *AtSec24C* expression in *atsec24bc* (+/*24b*, +/*24c*) plant, it needs that a construct for expression of *AtSec24C* are transformed into the *AtSec24B-GFP* transgenic *atsec24b-1* (*24b*/*24b*) plants. For this purpose, another selection marker that differs from that used in pre-existing transgenic plants is required, and it is beneficial if binary vector systems with a variety of selection markers are available for research use. Previously, Dr. Nakagawa *et al.* including the author constructed Gateway binary vector series for three different markers: neomycin phosphotransferase II (*NPTII*) for selection with kanamycin [14,15,43], hygromycin phosphotransferase (*HPT*) for selection with hygromycin [14,15,43], and phosphinothricin acetyltransferase (*bialaphos resistance gene*; *bar*) for selection with BASTA® [16]. All marker genes were driven by the nopaline synthase promoter (*Pnos*) and were followed by the nopaline synthase terminator (*Tnos*). Recently, Dr. Nozomu Koizumi *et al.* found that the GPT gene confers tunicamycin resistance on Arabidopsis when overexpressed by a P_{35S}, and Dr. Koizumi *et al.* made binary vector pZT4B containing P_{35S}*:GPT:Tnos* as a selection marker [77,78]. In the present study, the author chose the GPT gene as the fourth selection marker in the Gateway binary vector system, and made two new series of Gateway binary vectors carrying the *Pnos:GPT:Tnos* marker to avoid any possible influence of the P_{35S} sequence on the strength and expression pattern of the cloned gene [79]. The new series of Gateway binary vectors contained *att*R1-*att*R2 type (available for promoter analysis and ectopic expression of cDNA) and *att*R4-*att*R2 type (available for expression of cDNA with any combination of promoters) constructs. These vectors were named pGWB701-761s (*att*R1-*att*R2 type) and R4pGWB701-759s (*att*R4-*att*R2 type), where 7XXs indicates the tunicamycin

resistance marker and the last two digits represent the kind of reporter and tag common to all Gateway binary vectors developed previously. The author also examined the optimal concentration of tunicamycin to select transformed Arabidopsis plants possessing the *Pnos:GPT:Tnos* marker.

To construct the new Gateway binary vectors, plasmids were handled according to standard methods [80]. KOD DNA polymerase (TOYOBO) was used for PCR. All the adapters and primers used in this study are listed in Table 3-1. The regions amplified by PCR and ligation junctions were confirmed by sequencing for all vectors. The *Pnos:GPT:Tnos* marker was constructed as follows: The *GPT:Tnos* sequence was amplified by PCR using pZT4B [78] as template with *Pnos-GPT*-F and *Tnos*-R primers. The *Pnos* sequence was amplified by PCR using pYLTAC7 [81] as template with the *Pnos*-F and *Pnos-GPT*-R primers. These products were diluted, mixed, and subjected to a second PCR with the *Pnos*-F and *Tnos*-R primers to make *Pnos:GPT:Tnos*. Using this amplified product as template, the author introduced silent mutations to destroy the *Hind*III and *Sac*I sites in *GPT* by sequential recombinant PCR [82]. In the first recombinant PCR, the primer set *Pnos*-F and *GPT-mut-Sac*I-R and the primer set *GPT-mut-Sac*I-F and *Tnos*-R were used to destroy the *Sac*I site. In the second recombinant PCR, the primer set *Pnos*-F and *GPT-mut-Hind*III-R and the primer set *GPT-mut-Hind*III-F and *Tnos*-R were used to destroy the *Hind*III site. The resulting *Pnos:GPT:Tnos* fragment, consisting of modified *GPT*, was introduced into the *Swa*I site of pPZP-NosT-*Asc*I/*Swa*I [43] to make pGWB700 (*Pnos:GPT:Tnos*). Because pGWB700 was used as the backbone, the *GPT* of all the Gateway binary vectors reported here had silent mutations of GAG (Glu76) to GAA and of AAG (Lys189) to AAA. A medium containing 100 mg L^{-1} spectinomycin was used to select *E. coli* DH5α harboring these plasmids. The Gateway cassette and reporter/tag genes were introduced into pGWB700 as previously described [15,43,83] to make pGWB701-761s and R4pGWB701-759s. *E. coli* DB3.1 harboring these vectors was selected on a medium containing 100 mg L^{-1} of spectinomycin and 30 mg L^{-1} of chloramphenicol.

Table 3-1 Synthetic Oligonucleotides

Oligos	Sequence[a]
Pnos-GPT-F	5'-GGGGCAATAAGATATGGCAGCTCGTAAGA-3'
Pnos-GPT-R	5'-TCTTACGAGCTGCCATATCTTATTGCCCC-3'
Pnos-F	5'-CTATTAATCTCGACGGATCAGCTTCAC-3'
Tnos-R	5'-CTATTAATTCCCGATCTAGTAACATAG-3'
*GPT-mut-Sac*I-F	5'-TTGATAATGAACTCAAGCGA-3'
*GPT-mut-Sac*I-R	5'-TCGCTTGAGTTCATTATCAA-3'
*GPT-mut-Hind*III-F	5'-GGAGAGTAAAACTTGTCCTG-3'
*GPT-mut-Hind*III-R	5'-CAGGACAAGTTTTACTCTCC-3'
*ATRP62-pro-att*B1	5'-AAAAAGCAGGCTCCGACACTGATTTCTCTGGAAACAAACT-3'
*ATRP62-pro-att*B2	5'-AGAAAGCTGGGTAGACACTCATTATTTAAGCAAAGAGATGGA-3'

[a]Initiation codons (CAT in complementary orientation) in primers are underlined

Figure 3-1 shows the schematic structure of the pGWB701-761s and R4pGWB701-759s. All the vectors carried a *Pnos:GPT:Tnos* tunicamycin resistance marker placed in reverse orientation to the gene cloned by an LR reaction (Figure 3-1a). The structures around the Gateway cassette are classified in Fig. 1B. The pGWB701-761s (*att*R1-*att*R2 type) (Figure 3-1b, left panel) had the same type of Gateway cassettes as previously constructed ImpGWBs [43] and accepted *att*L1-(promoter and/or cDNA)-*att*L2 entry clones. R4pGWB701-759s (*att*R4-*att*R2 type) (Figure 3-1b, right panel) had the same type of Gateway cassettes as previously constructed R4pGWBs [15] and were available for promoter swapping combined with *att*L4-promoter-*att*R1 and *att*L1-cDNA-*att*L2 entry clones. Figure 3-1c shows the 16 reporters and tags employed in each vector. The last two digits of the vector number indicate the kinds and the positions of tag and reporter, like the previously constructed Gateway binary vectors [14-16,43,83,84]. The complete nucleotide sequences for pGWB701-761s and R4pGWB701-759s reported here appear in the GenBank/EMBL/DDBJ database under accession nos. AB608267 to AB608329. The linker sequences around the *att*B sites created after the LR reaction are the same as those previously reported [16].

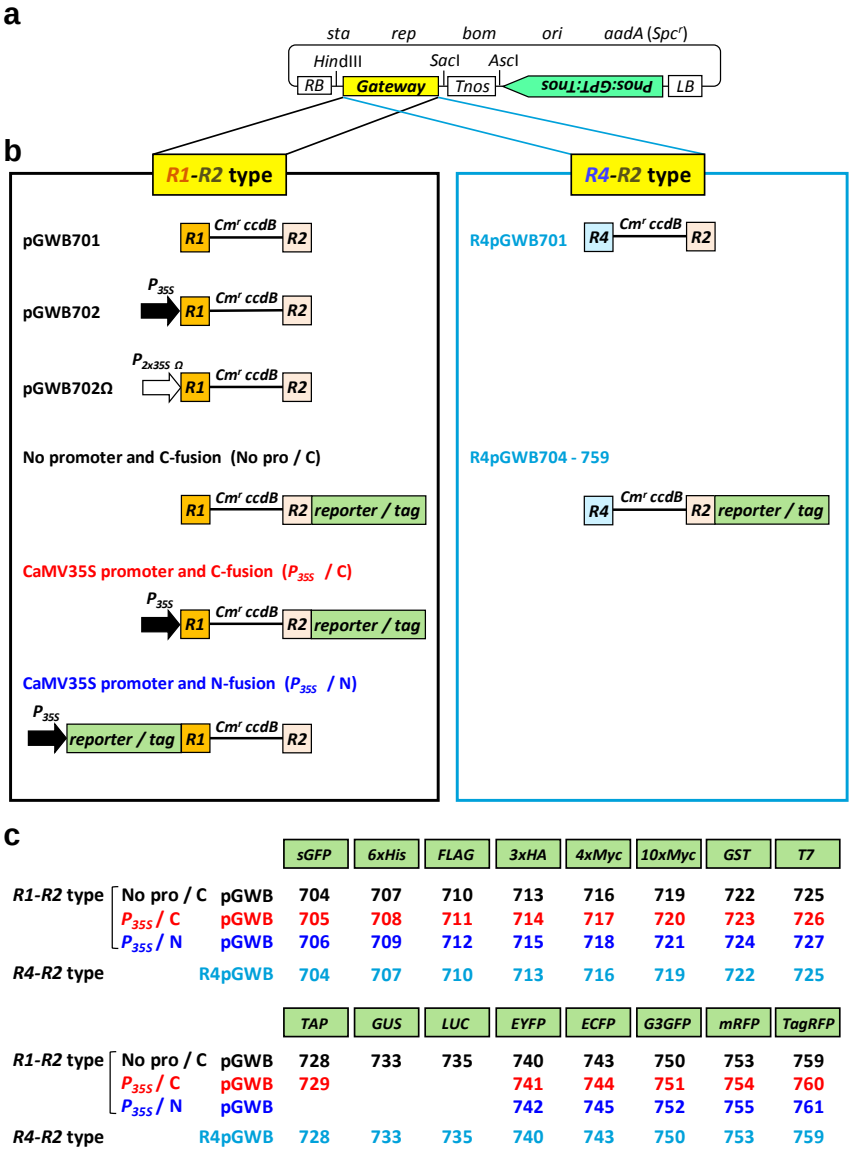

Fig. 3-1 Schematic Illustration of pGWB701-761 and R4pGWB701-759

a, All vectors contain the plant selection marker *Pnos:GPT:Tnos* in reverse orientation to the Gateway cassette. *RB*, right border; *LB*, left border; *sta*, region conferring stability in Agrobacterium tumefaciens; *rep*, broad host-range replication origin; *bom*, *cis*-acting element for conjugational transfer; *ori*, ColE1 replication origin; *aadA*, spectinomycin-resistance marker (Spc^r) used for selection in bacteria. **b**, The structure of the *Gateway* region in (**a**). The left panel shows the structures of vectors possessing an *att*R1-*att*R2 cassette (pGWB701-761). The right panel shows the structures of vectors possessing an *att*R4-*att*R2 cassette (R4pGWB701-759). *Cm*^{r}, chloramphenicol-resistance marker; *ccd*B, negative selection marker used in bacteria; R1, *att*R1; R2, *att*R2; R4, *att*R4. **c**, Reporters and tags employed in the pGWBs illustrated in (**b**). The vector number corresponds to the reporter/tag and type of fusion. sGFP, synthetic green fluorescent protein with S65T mutation [85,86]; 6xHis, hexahistidine tag; FLAG, FLAG-tag [87]; 3xHA, triple

HA tag [88]; 4xMyc and 10xMyc, four repeats and 10 repeats of the Myc tag respectively [88]; GST, glutathione S-transferase [89]; T7, T7-epitope tag [90]; TAP, tandem affinity purification [91]; GUS, β-glucuronidase [92]; LUC, modified luciferase, luc+ [93]; EYFP, enhanced yellow fluorescent protein [94]; ECFP, enhanced cyan fluorescent protein [94]; G3GFP, G3 green fluorescent protein [95]; mRFP, monomeric red fluorescent protein [96]; TagRFP, tag red fluorescent protein [97]

To test the performance of these vectors, pGWB733 was used for promoter:GUS analysis of the *A. thaliana* receptor protein 62 gene (*ATRP62*/*AtRLP27* [98]). *ATRP62* (At2g33060) encoded a leucine-rich repeat protein and was expressed dominantly in the stomata and trichomes (S. Nakamura, unpublished results). The promoter fragment spanning the sequence between –2,000 and +3 (A of the translational initiation codon was designated +1) of *ATRP62* was amplified from genomic DNA by adapter PCR with *ATRP62-pro-att*B1 and *ATRP62-pro-att*B2 primers shown in Table 3-1. The prepared fragment was cloned into pDONR201 (Life Technologies) by a BP reaction following the manufacturer's instructions (Life Technologies) to construct an *att*L1-*ATRP62 promoter-att*L2 entry clone. The entry clone was introduced into pGWB733 by an LR reaction following the manufacturer's instructions (Life Technologies) to make *ATRP62 promoter:GUS*. This construct was introduced into *A. tumefaciens* C58C1 (pMP90), and used in the transformation of *A. thaliana* (Col-0 accession) by a floral dip procedure [41]. Because the appropriate tunicamycin concentration for selection was not known for *Pnos*-driven GPT, T_0 seeds were plated on MS medium containing 0.025, 0.05, 0.075, 0.1, or 0.25 mg L^{-1} of tunicamycin (WAKO, Osaka, Japan). Resistant plants were distinguishable only on plates containing 0.25 mg L^{-1} of tunicamycin, but were severely damaged by an overdose of tunicamycin (data not shown). To confirm integration of the transgene, GUS staining was performed using excised leaves of resistant plants. Next, segregation of the transgene was examined by GUS staining of T_2 seedlings prepared from GUS-positive T_1 plants, and a line showing Mendelian characteristics was used in further study as a transgenic line carrying a single locus of the transgene. To determine the optimal tunicamycin concentration to select transformants possessing the *Pnos:GPT:Tnos* marker in a healthy condition, T_2 seeds were plated on medium containing 0, 0.1, 0.15, 0.2, or 0.25 mg L^{-1} of tunicamycin and were grown for 10 d at 22ºC. As shown in Figure 3-2a-h, resistant plants

were most clearly distinguishable on the plate containing 0.15 mg L^{-1} of tunicamycin. At this concentration, non-transformants were defective in root elongation and cotyledon spread after germination (Figure 3-2g, lower seedling) in contrast to the T_2 plants, which grew well on the same plate (Figure 3-2g, upper seedling). Primary screening of T_0 seeds was performed on a medium containing 0.15 mg L^{-1} of tunicamycin, and transformants were effectively selected at this concentration (Figure 3-2i). In average, 2 to 3% of resistant plants appeared on the selection plates, and all of those examined in this study were found to have the transgene by GUS staining. The optimal concentration of tunicamycin determined (0.15 mg L^{-1}) was lower than that stated in a previous report (0.3 mg L^{-1}) using pZB4B [78], perhaps because of the difference in promoters used for GPT in pGWB733 (*Pnos:GPT:Tnos*) and pZB4B (P_{35S}*:GPT:Tnos*). Figure 3-2j and k show the results of GUS staining of the T_2 seedlings. GUS expression was observed mainly in the stomata and trichomes.

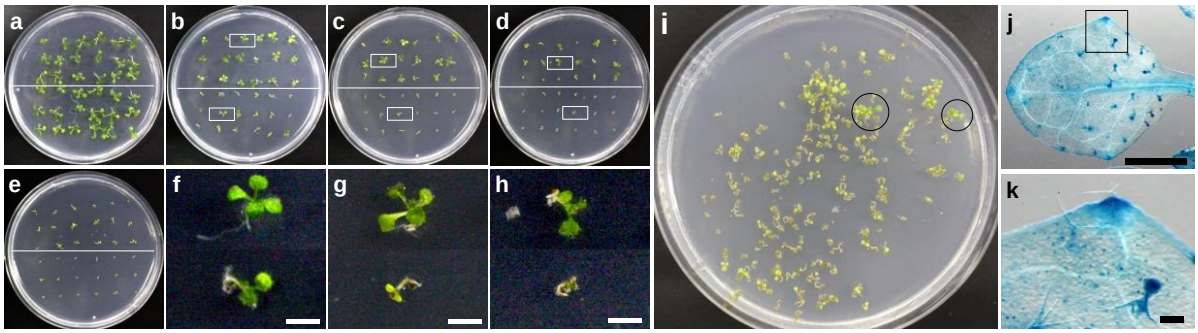

Fig. 3-2 Selection and analysis of transformants
a-f, Examination of the optimal tunicamycin concentration for selection of transformed Arabidopsis plants possessing the *Pnos:GPT:Tnos* marker. T_2 seeds (upper half of each plate) and wild-type seeds (lower half of each plate) were plated on media containing 0 (**a**), 0.1 (**b**), 0.15 (**c**), 0.2 (**d**), or 0.25 mg L^{-1} (**e**) tunicamycin, and were incubated for 10 d at 22ºC under continuous light. **f-h**, Magnified images of the indicated regions of **b**, **c**, and **d**, respectively. Tunicamycin-resistant T_2 (upper seedling) and wild-type (lower seedling). Bar = 3 mm. **i**, Primary screening of T_0 seeds on a plate containing 0.15 mg L^{-1} of tunicamycin. The plate was incubated for 2 weeks at 22º C under continuous light. Seedlings resistant to tunicamycin are circled. **j** and **k**, Histochemical analysis of GUS expression in leaves of T_2 Arabidopsis plants possessing the *ATRP62promoer :GUS* gene. **j**, Whole image of leaf (bar = 1 mm). **k**, Magnified image of the indicated region of **j** (bar = 0.1 mm)

In conclusion, the author developed two new series of Gateway binary vectors, pGWB701-761s and R4pGWB701-759s, possessing *Pnos:GPT:Tnos* as a selection marker, and determined the optimal tunicamycin concentration (0.15 mg L^{-1}) for transgenic experiments on Arabidopsis. pGWB701-761s and R4pGWB701-759s have the same backbone and reporter/tag sequences as previously constructed kanamycin [14,43], hygromycin [14,43], and BASTA® [16] resistance marker series, so many fusion genes using the desired selection marker can be constructed to carry out transgenic research under uniform conditions. In addition, the new vector series carrying selection marker *GPT* derived from plants might have advantages in practical use, since the Food and Agriculture Organization of the United Nations (FAO) has recommended not using selection markers derived from bacteria for the generation of transgenic crops. All the vectors described in this report will be made available for non-commercial research purposes, although the permission of the original developers will be required for some reporters.

Chapter 4

Proposed conclusions

A. thaliana is a powerful model organism for plant physiology, plant molecular biology, and plant genetics. The author revealed that two COPII component, AtSec24B and AtSec24C, are involved in gametogenesis of the *A. thaliana* in study of **Chapter 2**. At the same time, this study suggested the necessity of vectors enabling to introduce a transgene into pre-existing transgenic lines. In **Chapter 3**, the author developed Gateway binary vector series possessing a new selection marker. In this thesis, the author proposes the conclusions as follows:

(i) AtSec24B and AtSec24C, in addition to AtSec24A, are involved in protein transport as COPII components in *A. thaliana*.

AtSec24B and AtSec24C conserved the amino acid residues that contribute to the interaction with cargo. AtSec24B-GFP and AtSec24C-GFP showed dynamic subcellular distributions characteristic of COPII components in Arabidopsis epidermal cells.

(ii) AtSec24B and AtSec24C are redundantly involved in male and female gametogenesis.

A lack of AtSec24B led to mild male sterility with reduction of pollen germination. The significant decrease of AtSec24B and AtSec24C gave rise to the abortion of pollen at binuclear stage and the arrest of development in embryo sac among various stages.

(iii) The tunicamaycin resistant binary vectors are available for preparation of multi-transformants suitable to various researches with *A. thaliana*.

The author developed two new series of Gateway binary vectors, pGWB701-761s and R4pGWB701-759s, possessing *Pnos:GPT:Tnos* as a selection marker, and determined the optimal tunicamycin concentration (0.15 mg L^{-1}) for transgenic experiments on Arabidopsis. In the vectors, 16 kinds of reporter/tag are available.

References

1) Bowman J (1994) Arabidopsis: an atlas of morphology and development. Springer-Verlag, New York Inc.

2) Matsuoka K, Orci L, Amherdt M, Bednarek SY, Hamamoto S, Schekman R, and Yeung T (1998) COPII-coated vesicle formation reconstituted with purified coat proteins and chemically defined liposomes. *Cell* 93: 263-275

3) Sato K, and Nakano A (2007) Mechanisms of COPII vesicle formation and protein sorting. *FEBS Lett* 581: 2076-2082

4) Huang M, Weissman JT, Beraud-Dufour S, Luan P, Wang C, Chen W, Aridor M, Wilson IA, and Balch WE (2001) Crystal structure of Sar1-GDP at 1.7 Å resolution and the role of the NH_2 terminus in ER export. *J Cell Biol* 155: 937-948

5) Miller EA, Beilharz TH, Malkus PN, Lee MC, Hamamoto S, Orci L, and Schekman R (2003) Multiple cargo binding sites on the COPII subunit Sec24p ensure capture of diverse membrane proteins into transport vesicles. *Cell* 114: 497-509

6) Mossessova E, Bickford LC, and Goldberg J (2003) SNARE selectivity of the COPII coat. *Cell* 114: 483-495

7) Bi X, Corpina RA, and Goldberg J (2002) Structure of the Sec23/24-Sar1 pre-budding complex of the COPII vesicle coat. *Nature* 419: 271-277

8) Lederkremer GZ, Cheng Y, Petre BM, Vogan E, Springer S, Schekman R, Walz T, and Kirchhausen T (2001) Structure of the Sec23p/24p and Sec13p/31p complexes of COPII. *Proc Natl Acad Sci USA* 98: 10704-10709

9) Mancias JD, and Goldberg J (2007) The transport signal on Sec22 for packaging into COPII-coated vesicles is a conformational epitope. *Mol Cell* 26: 403-414

10) McCormick S (1993) Male Gametophyte Development. *Plant Cell* 5: 1265-1275

11) Christensen CA, King EJ, Jordan JR, and Drews GN (1997) Megagametogenesis in *Arabidopsis* wild type and the *Gf* mutant. *Sex Plant Reprod* 10: 49-64

12) Yadegari R, and Drews GN (2004) Female gametophyte development. *Plant Cell* 16 Suppl: S133-141

13) Walhout AJ, Temple GF, Brasch MA, Hartley JL, Lorson MA, van den Heuvel S, and Vidal M (2000) GATEWAY recombinational cloning: application to the cloning of large numbers of open reading frames or ORFeomes. *Methods Enzymol* 328: 575-592

14) Nakagawa T, Ishiguro S, and Kimura T (2009) Gateway vectors for plant transformation. *Plant Biotechnol* 26: 275-284

15) Nakagawa T, Nakamura S, Tanaka K, Kawamukai M, Suzuki T, Nakamura K, Kimura T, and Ishiguro S (2008) Development of R4 Gateway Binary Vectors (R4pGWB) Enabling High-Throughput Promoter Swapping for Plant Research. *Biosci Biotechnol Biochem* 72: 624-629

16) Nakamura S, Mano S, Tanaka Y, Ohnishi M, Nakamori C, Araki M, Niwa T, Nishimura M, Kaminaka H, Nakagawa T, Sato Y, and Ishiguro S (2010) Gateway Binary Vectors with the Bialaphos Resistance Gene, bar, as a Selection Marker for Plant Transformation. *Biosci Biotechnol Biochem* 74: 1315-1319

17) Heifetz A, Keenan RW, and Elbein AD (1979) Mechanism of action of tunicamycin on UDP-GlcNAc:dolichyl-phosphate GlcNAc-1-phospate

transferase. *Biochemistry* 18: 2186-2192

18) Takatsuki A, Kawamura K, Okina M, Kodama Y, Ito T, and Tamura G (1977) The structure of tunicamycin. *Agric Biol Chem* 41: 2307-2309

19) Schekman R, and Orci L (1996) Coat proteins and vesicle budding. *Science* 271: 1526-1533

20) Barlowe C, and Schekman R (1993) *SEC12* encodes a guanine-nucleotide-exchange factor essential for transport vesicle budding from the ER. *Nature* 365: 347-349

21) Nakano A, Brada D, and Schekman R (1988) A membrane glycoprotein, Sec12p, required for protein transport from the endoplasmic reticulum to the Golgi apparatus in yeast. *J Cell Biol* 107: 851-863

22) Sato M, Sato K, and Nakano A (1996) Endoplasmic reticulum localization of Sec12p is achieved by two mechanisms: Rer1p-dependent retrieval that requires the transmembrane domain and Rer1p-independent retention that involves the cytoplasmic domain. *J Cell Biol* 134: 279-293

23) Kuehn MJ, Herrmann JM, and Schekman R (1998) COPII-cargo interactions direct protein sorting into ER-derived transport vesicles. *Nature* 391: 187-190

24) Yoshihisa T, Barlowe C, and Schekman R (1993) Requirement for a GTPase-activating protein in vesicle budding from the endoplasmic reticulum. *Science* 259: 1466-1468

25) Miller E, Antonny B, Hamamoto S, and Schekman R (2002) Cargo selection into COPII vesicles is driven by the Sec24p subunit. *EMBO J* 21: 6105-6113

26) Miller EA, Liu Y, Barlowe C, and Schekman R (2005) ER-Golgi transport defects are associated with mutations in the Sed5p-binding domain of the COPII coat subunit, Sec24p. *Mol Biol Cell* 16: 3719-3726

27) Phillipson BA, Pimpl P, daSilva LL, Crofts AJ, Taylor JP, Movafeghi A, Robinson DG, and Denecke J (2001) Secretory bulk flow of soluble proteins is efficient and COPII dependent. *Plant Cell* 13: 2005-2020

28) Takeuchi M, Ueda T, Sato K, Abe H, Nagata T, and Nakano A (2000) A dominant negative mutant of Sar1 GTPase inhibits protein transport from the endoplasmic reticulum to the Golgi apparatus in tobacco and *Arabidopsis* cultured cells. *Plant J* 23: 517-525

29) daSilva LL, Snapp EL, Denecke J, Lippincott-Schwartz J, Hawes C, and Brandizzi F (2004) Endoplasmic reticulum export sites and Golgi bodies behave as single mobile secretory units in plant cells. *Plant Cell* 16: 1753-1771

30) Stefano G, Renna L, Chatre L, Hanton SL, Moreau P, Hawes C, and Brandizzi F (2006) In tobacco leaf epidermal cells, the integrity of protein export from the endoplasmic reticulum and of ER export sites depends on active COPI machinery. *Plant J* 46: 95-110

31) Yang YD, Elamawi R, Bubeck J, Pepperkok R, Ritzenthaler C, and Robinson DG (2005) Dynamics of COPII vesicles and the Golgi apparatus in cultured *Nicotiana tabacum* BY-2 cells provides evidence for transient association of Golgi stacks with endoplasmic reticulum exit sites. *Plant Cell* 17: 1513-1531

32) Hanton SL, Matheson LA, Chatre L, and Brandizzi F (2009) Dynamic organization of COPII coat proteins at endoplasmic reticulum export sites in plant cells. *Plant J* 57: 963-974

33) Westphal S, Soll J, and Vothknecht UC (2001) A vesicle transport system inside chloroplasts. *FEBS Lett* 506: 257-261

34) Andersson MX, and Sandelius AS (2004) A chloroplast-localized vesicular transport system: a bio-informatics approach. *BMC Genomics* 5: 40

35) Hanton SL, Chatre L, Renna L, Matheson LA, and Brandizzi F (2007) De novo formation of plant endoplasmic reticulum export sites is membrane cargo induced and signal mediated. *Plant Physiol* 143: 1640-1650

36) Sieben C, Mikosch M, Brandizzi F, and Homann U (2008) Interaction of the K^+-channel KAT1 with the coat protein complex II coat component Sec24 depends on a di-acidic endoplasmic reticulum export motif. *Plant J* 56: 997-1006

37) Faso C, Chen YN, Tamura K, Held M, Zemelis S, Marti L, Saravanan R, Hummel E, Kung L, Miller E, Hawes C, and Brandizzi F (2009) A missense mutation in the *Arabidopsis* COPII coat protein Sec24A induces the formation of clusters of the endoplasmic reticulum and Golgi apparatus. *Plant Cell* 21: 3655-3671

38) Nakano RT, Matsushima R, Ueda H, Tamura K, Shimada T, Li L, Hayashi Y, Kondo M, Nishimura M, and Hara-Nishimura I (2009) GNOM-LIKE1/ERMO1 and SEC24a/ERMO2 are required for maintenance of endoplasmic reticulum morphology in *Arabidopsis thaliana*. *Plant Cell* 21: 3672-3685

39) Conger R, Chen Y, Fornaciari S, Faso C, Held MA, Renna L, and Brandizzi F (2011) Evidence for the involvement of the *Arabidopsis* SEC24A in male transmission. *J Exp Bot* 62: 4917-4926

40) Hino T, Tanaka Y, Kawamukai M, Nishimura K, Mano S, and Nakagawa T (2011) Two Sec13p homologs, AtSec13A and AtSec13B, redundantly contribute to the formation of COPII transport vesicles in *Arabidopsis thaliana*. *Biosci Biotechnol Biochem* 75: 1848-1852

41) Clough SJ, and Bent AF (1998) Floral dip: a simplified method for *Agrobacterium*-mediated transformation of *Arabidopsis thaliana*. *Plant J* 16: 735-743

42) Nakamura S, Suzuki T, Kawamukai M, and Nakagawa T (2012) Expression analysis of *Arabidopsis thaliana* small secreted protein genes. *Biosci Biotechnol Biochem* 76: 436-446

43) Nakagawa T, Suzuki T, Murata S, Nakamura S, Hino T, Maeo K, Tabata R, Kawai T, Tanaka K, Niwa Y, Watanabe Y, Nakamura K, Kimura T, and Ishiguro S (2007) Improved Gateway binary vectors: high-performance vectors for creation of fusion constructs in transgenic analysis of plants. *Biosci Biotechnol Biochem* 71: 2095-2100

44) Boavida LC, and McCormick S (2007) Temperature as a determinant factor for increased and reproducible *in vitro* pollen germination in *Arabidopsis thaliana*. *Plant J* 52: 570-582

45) Lee Y, Kim ES, Choi Y, Hwang I, Staiger CJ, and Chung YY (2008) The Arabidopsis phosphatidylinositol 3-kinase is important for pollen development. *Plant Physiol* 147: 1886-1897

46) Robinson DG, Herranz MC, Bubeck J, Pepperkok R, and Ritzenthaler C (2007) Membrane dynamics in the early secretory pathway. *Crit Rev Plant Sci* 26: 199-225

47) Belles-Boix E, Babiychuk E, Montagu MV, Inze D, and Kushnir S (2000) CEF, a Sec24 homologue of *Arabidopsis thaliana*, enhances the survival of yeast under oxidative stress conditions. *J Exp Bot* 51: 1761-1762

48) Peng R, Grabowski R, De Antoni A, and Gallwitz D (1999) Specific interaction of the yeast *cis*-Golgi syntaxin Sed5p and the coat protein complex II component Sec24p of endoplasmic reticulum-derived transport vesicles. *Proc Natl Acad Sci USA* 96: 3751-3756

49) Uemura T, Ueda T, Ohniwa RL, Nakano A, Takeyasu K, and Sato MH (2004) Systematic analysis of SNARE molecules in *Arabidopsis*: dissection of the post-Golgi network in plant cells. *Cell Struct Funct* 29: 49-65

50) Bubeck J, Scheuring D, Hummel E, Langhans M, Viotti C, Foresti O, Denecke J, Banfield DK, and Robinson DG (2008) The syntaxins SYP31 and SYP81 control ER-Golgi trafficking in the plant secretory pathway. *Traffic* 9: 1629-1652

51) Chatre L, Brandizzi F, Hocquellet A, Hawes C, and Moreau P (2005) Sec22 and Memb11 are v-SNAREs of the anterograde endoplasmic reticulum-Golgi pathway in tobacco leaf epidermal cells. *Plant Physiol* 139: 1244-1254

52) Boevink P, Oparka K, Santa Cruz S, Martin B, Betteridge A, and Hawes C (1998) Stacks on tracks: the plant Golgi apparatus traffics on an actin/ER network. *Plant J* 15: 441-447

53) Alexander MP (1969) Differential staining of aborted and nonaborted pollen. *Stain Technol* 44: 117-122

54) Schnurr JA, Storey KK, Jung HJ, Somers DA, and Gronwald JW (2006) UDP-sugar pyrophosphorylase is essential for pollen development in Arabidopsis. *Planta* 224: 520-532

55) Toller A, Brownfield L, Neu C, Twell D, and Schulze-Lefert P (2008) Dual function of Arabidopsis glucan synthase-like genes *GSL8* and *GSL10* in male gametophyte development and plant growth. *Plant J* 54: 911-923

56) Preuss D, Rhee SY, and Davis RW (1994) Tetrad analysis possible in *Arabidopsis* with mutation of the *QUARTET* (*QRT*) genes. *Science* 264: 1458-1460

57) Smyth DR, Bowman JL, and Meyerowitz EM (1990) Early flower development in *Arabidopsis*. *Plant Cell* 2: 755-767

58) Christensen CA, Subramanian S, and Drews GN (1998) Identification of gametophytic mutations affecting female gametophyte development in

Arabidopsis. *Dev Biol* 202: 136-151

59) Pagano A, Letourneur F, Garcia-Estefania D, Carpentier JL, Orci L, and Paccaud JP (1999) Sec24 proteins and sorting at the endoplasmic reticulum. *J Biol Chem* 274: 7833-7840

60) Kuang A, and Musgrave ME (1996) Dynamics of vegetative cytoplasm during generative cell formation and pollen maturation in *Arabidopsis thaliana*. *Protoplasma* 194: 81-90

61) Owen HA, and Makaroff CA (1995) Ultrastructure of microsporogenesis and microgametogenesis in *Arabidopsis thaliana* (L.) Heynh. ecotype Wassilewskija (Brassicaceae). *Protoplasma* 185: 7-21

62) Park SK, and Twell D (2001) Novel patterns of ectopic cell plate growth and lipid body distribution in the Arabidopsis *gemini pollen1* mutant. *Plant Physiol* 126: 899-909

63) Yamamoto Y, Nishimura M, Hara-Nishimura I, and Noguchi T (2003) Behavior of vacuoles during microspore and pollen development in *Arabidopsis thaliana*. *Plant Cell Physiol* 44: 1192-1201

64) Brown RC, and Lemmon BE (1991) Pollen development in orchids.5. A generative cell domain involved in spatial control of the hemispherical cell plate. *J Cell Sci* 100: 559-565

65) Samuels AL, Giddings TH, and Staehelin LA (1995) Cytokinesis in tobacco BY-2 and root-tip cells: a new model of cell plate formation in higher plants. *J Cell Biol* 130: 1345-1357

66) Otegui MS, and Staehelin LA (2004) Electron tomographic analysis of post-meiotic cytokinesis during pollen development in *Arabidopsis thaliana*. *Planta* 218: 501-515

67) Verma DP (2001) Cytokinesis and building of the cell plate in plants. *Annu Rev Plant Physiol Plant Mol Biol* 52: 751-784

68) Dong X, Hong Z, Sivaramakrishnan M, Mahfouz M, and Verma DP (2005) Callose synthase (CalS5) is required for exine formation during microgametogenesis and for pollen viability in Arabidopsis. *Plant J* 42: 315-328

69) Xie B, Deng Y, Kanaoka MM, Okada K, and Hong Z (2012) Expression of *Arabidopsis* callose synthase 5 results in callose accumulation and cell wall permeability alteration. *Plant Sci* 183: 1-8

70) Pagnussat GC, Yu HJ, Ngo QA, Rajani S, Mayalagu S, Johnson CS, Capron A, Xie LF, Ye D, and Sundaresan V (2005) Genetic and molecular identification of genes required for female gametophyte development and function in *Arabidopsis*. *Development* 132: 603-614

71) El-Kasmi F, Pacher T, Strompen G, Stierhof YD, Muller LM, Koncz C, Mayer U, and Jurgens G (2011) Arabidopsis SNARE protein SEC22 is essential for gametophyte development and maintenance of Golgi-stack integrity. *Plant J* 66: 268-279

72) Li N, Yuan L, Liu N, Shi D, Li X, Tang Z, Liu J, Sundaresan V, and Yang WC (2009) *SLOW WALKER2*, a NOC1/MAK21 homologue, is essential for coordinated cell cycle progression during female gametophyte development in Arabidopsis. *Plant Physiol* 151: 1486-1497

73) Shi DQ, Liu J, Xiang YH, Ye D, Sundaresan V, and Yang WC (2005) *SLOW WALKER1*, essential for gametogenesis in Arabidopsis, encodes a WD40 protein involved in 18S ribosomal RNA biogenesis. *Plant Cell* 17: 2340-2354

74) Mano S, Miwa T, Nishikawa S, Mimura T, and Nishimura M (2007) The plant organelles database (PODB): a collection of visualized plant organelles and protocols for plant organelle research. *Nucl Acids Res* 36: D929-D937

75) Azpiroz-Leehan R, and Feldmann KA (1997) T-DNA insertion

mutagenesis in Arabidopsis: going back and forth. *Trends Genet.* 13: 152-156

76) Alonso JM, Stepanova AN, Leisse TJ, Kim CJ, Chen H, Shinn P, Stevenson DK, Zimmerman J, Barajas P, Cheuk R, Gadrinab C, Heller C, Jeske A, Koesema E, Meyers CC, Parker H, Prednis L, Ansari Y, Choy N, Deen H, Geralt M, Hazari N, Hom E, Karnes M, Mulholland C, Ndubaku R, Schmidt I, Guzman P, Aguilar-Henonin L, Schmid M, Weigel D, Carter DE, Marchand T, Risseeuw E, Brogden D, Zeko A, Crosby WL, Berry CC, and Ecker JR (2003) Genome-wide insertional mutagenesis of *Arabidopsis thaliana*. *Science* 301: 653-657

77) Koizumi N (2003) A chimeric tunicamycin resistance gene as a new selectable marker for *Arabidopsis thaliana*. *Plant Biotechnol* 20: 305-309

78) Koizumi N, and Iwata Y (2008) Construction of a Binary Vector for Transformation of *Arabidopsis thaliana* with a New Selection Marker. *Biosci Biotechnol Biochem* 72: 3041-3043

79) Zheng X, Deng W, Luo K, Duan H, Chen Y, McAvoy R, Song S, Pei Y, and Li Y (2007) The cauliflower mosaic virus (CaMV) 35S promoter sequence alters the level and patterns of activity of adjacent tissue- and organ-specific gene promoters. *Plant Cell Rep* 26: 1195-1203

80) Sambrook J, and Russell D (2001) Molecular Cloning, a Laboratory Manual. Cold Spring Harbor Laboratory Press, Cold Spring Harbor

81) Liu YG, Shirano Y, Fukaki H, Yanai Y, Tasaka M, Tabata S, and Shibata D (1999) Complementation of plant mutants with large genomic DNA fragments by a transformation-competent artificial chromosome vector accelerates positional cloning. *Proc Natl Acad Sci USA* 96: 6535-6540

82) Higuchi R (1990) PCR Protocols A Guide to Methods and Applications. Academic Press, Inc., San Diego, California

83) Nakamura S, Nakao A, Kawamukai M, Kimura T, Ishiguro S, and Nakagawa T (2009) Development of Gateway binary vectors, R4L1pGWBs, for promoter analysis in higher plants. *Biosci Biotechnol Biochem* 73: 2556-2559

84) Nakagawa T, Kurose T, Hino T, Tanaka K, Kawamukai M, Niwa Y, Toyooka K, Matsuoka K, Jinbo T, and Kimura T (2007) Development of series of gateway binary vectors, pGWBs, for realizing efficient construction of fusion genes for plant transformation. *J Biosci Bioeng* 104: 34-41

85) Chiu W, Niwa Y, Zeng W, Hirano T, Kobayashi H, and Sheen J (1996) Engineered GFP as a vital reporter in plants. *Curr Biol* 6: 325-330

86) Niwa Y (2003) A synthetic green fluorescent protein gene for plant biotechnology. *Plant Biotechnol* 20: 1-11

87) Chubet RG, and Brizzard BL (1996) Vectors for expression and secretion of FLAG epitope-tagged proteins in mammalian cells. *Biotechniques* 20: 136-141

88) Bahler J, Wu JQ, Longtine MS, Shah NG, McKenzie A, 3rd, Steever AB, Wach A, Philippsen P, and Pringle JR (1998) Heterologous modules for efficient and versatile PCR-based gene targeting in *Schizosaccharomyces pombe*. *Yeast* 14: 943-951

89) Smith DB, and Johnson KS (1988) Single-step purification of polypeptides expressed in *Escherichia coli* as fusions with glutathione *S*-transferase. *Gene* 67: 31-40

90) Yano D, Sato M, Saito C, Sato MH, Morita MT, and Tasaka M (2003) A SNARE complex containing SGR3/AtVAM3 and ZIG/VTI11 in gravity-sensing cells is important for *Arabidopsis* shoot gravitropism. *Proc Natl Acad Sci USA* 100: 8589-8594

91) Rigaut G, Shevchenko A, Rutz B, Wilm M, Mann M, and Seraphin B

(1999) A generic protein purification method for protein complex characterization and proteome exploration. *Nat Biotechnol* 17: 1030-1032

92) Jefferson RA, Kavanagh TA, and Bevan MW (1987) GUS fusions: β-glucuronidase as a sensitive and versatile gene fusion marker in higher plants. *EMBO J* 6: 3901-3907

93) Sherf BA, and Wood KV (1994) Firefly luciferase engineered for improved genetic reporting. *Promega Notes* 49: 14-21

94) Huang J, Taylor JP, Chen JG, Uhrig JF, Schnell DJ, Nakagawa T, Korth KL, and Jones AM (2006) The plastid protein THYLAKOID FORMATION1 and the plasma membrane G-protein GPA1 interact in a novel sugar-signaling mechanism in *Arabidopsis*. *Plant Cell* 18: 1226-1238

95) Kawakami S, and Watanabe Y (1997) Use of green fluorescent protein as a molecular tag of protein movement *in vivo*. *Plant Biotechnol* 14: 127-130

96) Campbell RE, Tour O, Palmer AE, Steinbach PA, Baird GS, Zacharias DA, and Tsien RY (2002) A monomeric red fluorescent protein. *Proc Natl Acad Sci USA* 99: 7877-7882

97) Merzlyak EM, Goedhart J, Shcherbo D, Bulina ME, Shcheglov AS, Fradkov AF, Gaintzeva A, Lukyanov KA, Lukyanov S, Gadella TW, and Chudakov DM (2007) Bright monomeric red fluorescent protein with an extended fluorescence lifetime. *Nat. Methods* 4: 555-557

98) Wang G, Ellendorff U, Kemp B, Mansfield JW, Forsyth A, Mitchell K, Bastas K, Liu CM, Woods-Tor A, Zipfel C, de Wit PJ, Jones JD, Tor M, and Thomma BP (2008) A genome-wide functional investigation into the roles of receptor-like proteins in Arabidopsis. *Plant Physiol* 147: 503-517

List of Publications

Chapter 2

Yuji Tanaka・Kohji Nishimura・Makoto Kawamukai・Akinobu Oshima・Tsuyoshi Nakagawa (2013)
Redundant function of two Arabidopsis COPII components, AtSec24B and AtSec24C, is essential for male and female gametogenesis
Accepted for publication in *Planta*.
Online published: 19 June 2013.

Chapter 3

Yuji TANAKA, Shinya NAKAMURA, Makoto KAWAMUKAI, Nozomu KOIZUMI, and Tsuyoshi NAKAGAWA (2011)
Development of a Series of Gateway Binary Vectors Possessing a Tunicamycin Resistance Gene as a Marker for the Transformation of *Arabidopsis thaliana*
Bioscience Biotechnology and Biochemistry, 75 (4), 804-807, 2011.

Related Papers

Shinya NAKAMURA, Shoji MANO, Yuji TANAKA, Masato OHNISHI, Chihiro NAKAMORI, Masami ARAKI, Tomoko NIWA, Mikio NISHIMURA, Hironori KAMINAKA, Tsuyoshi NAKAGAWA, Yutaka SATO, and Sumie ISHIGURO (2010)
Gateway Binary Vectors with the Bialaphos Resistance Gene, *bar*, as a Selection Marker for Plant Transformation
Bioscience, Biotechnology, and Biochemistry, 74 (6), 1315-1319

Takeshi HINO, Yuji TANAKA, Makoto KAWAMUKAI, Kohji NISHIMURA, Shoji MANO, and Tsuyoshi NAKAGAWA (2011)
Two Sec13p Homologs, AtSec13A and AtSec13B, Redundantly Contribute to the Formation of COPII Transport Vesicles in *Arabidopsis thaliana*
Bioscience, Biotechnology, and Biochemistry, 75 (9), 1848-1852

Tetsuya KIMURA, Akihide NAKAO, Sachiko MURATA, Yasuyuki KOBAYASHI, Yuji TANAKA, Kenta SHIBAHARA, Tetsu KAWAZU, and Tsuyoshi NAKAGAWA (2013)
Development of the Gateway Recycling Cloning System for Multiple Linking of Expression Cassettes in a Defined Order, and Direction on Gateway Compatible Binary Vectors
Bioscience, Biotechnology, and Biochemistry, 77 (2), 430-434

Acknowledgments

The author would like to express his profound gratitude to Professor Dr. Tsuyoshi Nakagawa, Department of Molecular and Functional Genomics, Center for Integrated Research in Science, Shimane University, for his accurate guidance, valuable suggestion, and warm encouragement throughout the course of this work.

The author would like to express his grateful acknowledgement to Professor Dr. Makoto Kawamukai, Department of Life Science and Biotechnology, Shimane University, for his kind guidance, useful advice, and warm encouragement throughout the course of this work.

The author would like to express his gratitude to Associate Professor Dr. Tomohiro Kaino, Department of Life Science and Biotechnology, Shimane University, for his kind guidance and continuous encouragement throughout the course of this work.

The author would like to express his gratitude to Assistant Professor Dr. Kohji Nishimura, Department of Molecular and Functional Genomics, Center for Integrated Research in Science, Shimane University, for his technical guidance, useful advice, and warm encouragement throughout the course of this work.

The author would like to express his special thanks to Assistant Professor Dr. Yasuhiro Matsuo, Department of Life Science and Biotechnology, Shimane University, for his kind guidance and continuous encouragement throughout the course of this work.

The author would like to express his special thanks to Emeritus Professor Dr. Hideki Matsuda, Department of Applied Bioscience and Biotechnology, Shimane University, for his kind guidance.

The author would like to express his acknowledgment to Associate Professor Dr. Akinobu Oshima, Department of Biological Science, Shimane University, for his technical guidance.

The author would like to his thanks to Mr. Takeshi Hino, Dr. Shinya Nakamura, Mr. Tomio Taguchi, Ms. Erika Hotta, Ms. Mizuki Nohara, and Ms. Kimika Miyake, for their technical advice, warm support, and great help.

The author would like to express his thanks to his colleagues, Dr. Hiroaki Kato, Dr. Yasuo Oowatari, Dr. Yuzy Matsuo, Mr. Kazuhiro Hayashi, Dr. Katsuhiro Tanae, Mr. Yuya Akasaka, Mr. Tomitaka Horiuchi, Mr. Akihide Nakao, Mr. Kenta Shibahara, Mr. Masataka Ioka, Ms. Tomomi Oda, Ms. Chisato Yamada, and other members of the Laboratory of Life Science and Biotechnology in Shimane University.

Summary

In eukaryotic cells, the proteins synthesized on endoplasmic reticulum (ER) membrane are transported through the secretory pathway into each destined organelle or extracellular space and play important roles in cell activity. Anterograde protein transport from the ER to the Golgi apparatus, that is the start of the secretory pathway, is mediated by coat protein complex II (COPII)-coated vesicles. The COPII is composed of a small GTP-binding protein Sar1 and two coat protein complexes (Sec23/24 and Sec13/31). The COPII vesicle formation is achieved by continuous assembly of these coat proteins. When Sar1 is activated, the activated Sar1 is concurrently anchored into ER membrane. Sec23/24 complex is recruited from cytoplasm onto ER membrane to form a “prebudding complex” with Sar1 and selectively captures cargo proteins destined for incorporation into the COPII vesicle. Sec13/31 complex deforms the ER membrane and concentrates the cargo into the COPII vesicle by cross-linking the adjacent prebudding complexes, which leads to the completion of vesicle budding. In this process, Sec24 is thought to sort the cargo destined to be incorporated into the vesicle by immediate interaction with cargo. This knowledge has obtained from studies using the yeast and mammal cells. In plant cells, this transport system using the vesicle is conserved.

It has been known that *Arabidopsis thaliana* has three Sec24 homologs (AtSec24A, AtSec24B, and AtSec24C). Although only AtSec24A has been characterized, only sequence information was known for AtSec24B and AtSec24C. The author determined DNA sequence of CDS for AtSec24B and AtSec24C. The sequence results indicated that *AtSec24B* and *AtSec24C* conserve the domains characteristic of Sec24 family. The expression pattern and subcellular localization analysis using reporter proteins suggested that all of AtSec24s express in most of tissues and show distribution characteristic of COPII components in Arabidopsis epidermal cells. To reveal the biological functions of AtSec24B and AtSec24C in plant development, the author isolated an AtSec24B knockout line (*atsec24b-1*) and an AtSec24C knockdown line (*atsec24c-1*). *atsec24b-1*, but not *atsec24c-1*, showed mild male sterility with reduction of pollen germination. The experiments with cross between *atsec24b-1* and *atsec24c-1* suggested that significant decrease of AtSec24B and AtSec24C lead to abortion of pollen at binuclear stage and arrest of development in embryo sac among various stages.

Next, the author developed Gateway binary vectors possessing a new selection marker enabling to make multi-transformant. A large number of experimentally useful transgenic plants have been established. The introduction of a transgene into these pre-existing transgenic lines is an important method. For example, in above experiments, the T-DNA inserted in *atsec24b-1* and *atsec24c-1* possess kanamycin resistance marker, and the transformation using the binary vector (R4pGWB550) carrying hygromycin resistance marker performed for complementation of *atsec24b-1* lines. To complement the decrease of *AtSec24B* and *AtSec24C* expression in *atsec24bc* (+/*24b*, +/*24c*) plant, it needs that a construct for expressing *AtSec24C* are retransformed into the *atsec24bc* plant had already been complemented for *atsec24b-1*. UDP-N-acetylgulucosamine: dolichol phosphate N-acetylglucosamine-1-P transferase (GPT) is involved in synthesis of oligosaccharide for glycoprotein. In *A. thaliana*, Overexpression of the GPT confers tolerance to tunicamycin which is an inhibitor for the oligosaccharide synthesis. The author developed Gateway binary vectors possessing the GPT gene as a new selection marker for plant transformation. Like existing pGWB series, this vector series employs two recombination systems, in which 16 kinds of reporter/epitope tag are available. The result in the performance test of these vectors indicated that transformants are effectively selected on a medium containing 0.15 mg L^{-1} of tunicamycin.

From these results, it was revealed that AtSec24B and AtSec24C function as COPII in *A. thaliana* and are redundantly involved in male and female gametogenesis. The developed tunicamaycin resistant binary vectors are available for preparation of multi-transformants suitable to various plant researches.

要旨

真核細胞において小胞体(ER)膜上で合成されたタンパク質は分泌経路を経てそれぞれに定められた細胞内または細胞外区画へ運搬され、細胞活動に重要な役割を果たしている。分泌経路の初発であるERからゴルジ体へのタンパク質輸送はcoat protein complex II (COPII)に覆われた膜小胞が担っている。そのCOPIIは低分子量GTP結合タンパク質であるSar1と2種類のタンパク質複合体(Sec23/24複合体, Sec13/31複合体)から構成される。小胞の形成はこれらのタンパク質の連続的な会合によって起こる。まずSar1がGTPと結合することによって活性化され、ER膜上に結合する。この活性型Sar1を目印としてSec23/24複合体が集合し、同時に小胞内に取り込まれるべきタンパク質(積荷)を選択的に捉え、出芽前複合体を形成する。さらに、この出芽前複合体どうしをSec13/31複合体が架橋することにより、膜の湾曲が進み小胞の出芽が起こる。Sec24は積荷と直接結合することで、COPII小胞に取り込むべき積荷の認識を行っていると考えられている。このようなCOPII小胞を用いたタンパク質輸送は酵母や哺乳類細胞を用いた研究によって明らかにされており、植物においても保存されていることが示されている。

シロイヌナズナのゲノムには3種類のSec24ホモログ(AtSec24A, 24Bと24C)が存在することが知られている。AtSec24Aの機能はよく特徴づけられているが、AtSec24Bと24Cは塩基配列が予想されているのみである。そこで、著者は*AtSec24B*と*24C*の塩基配列を決定した。その結果、AtSec24Bと24CはSec24ファミリーに特徴的なドメインが保存されていることが示された。また、3種類のSec24ホモログ（AtSec24s）についてレポーターを用いた発現部位解析と細胞内局在解析を行った。その結果、すべてのAtSec24が細胞内でCOPIIに特徴的な分布を示し、ほとんどの組織で発現することが示された。さらに、シロイヌナズナの発達におけるAtSec24Bと24Cの機能を明らかにするために、AtSec24Bノックアウト株(*atsec24b-1*)とAtSec24Cノックダウン株(*atsec24c-1*)を単離した。*atsec24c-1*は異常を示さなかったが、*atsec24b-1*では花粉管の発芽率の低下が示された。また、それらの株の交配によって、AtSec24Bと24Cの著しい減少が雄性配偶体である花粉で第一有糸分裂後の発達停止を引き起こし、雌性配偶体である胚嚢においても様々な段階での発達停止を引き起こすことが示唆された。

次に、著者は多重形質転換が可能な新規薬剤耐性マーカーを持ったGatewayバイナリーベクターの開発を行った。現在、植物研究の進展によって様々な遺伝子導入植物が作製されており、既存の遺伝子導入植物にさらに遺伝子導入を行うことが必要となっている。例えば、上記の実験において、*atsec24b-1*と*atsec24c-1*は破壊株選抜マーカーとしてカナマイシン耐性遺伝子を有しており、*atsec24b-1*の相補のためにハイグロマイシン耐性遺伝子をもったベクターを用いて形質転換体を作製した。*atsec24b-1*と*atsec24c-1*の交配株を相補させるためにその形質転換体にさらに*AtSec24C*を

導入しようとした場合、カナマイシンやハイグロマイシンとは異なった薬剤に対する選抜マーカーをもったベクターを用いる必要がある。糖タンパク質の糖鎖合成に関与するUDP-*N*-acetylgulucosamine: dolichol phosphate *N*-acetylglucosamine-1-P transferase (GPT)は、シロイヌナズナで高発現されることによって、糖鎖合成の阻害剤であるツニカマイシンに対して抵抗性を与えることが知られている。そこで、著者は新たな選抜マーカーとしてGPT遺伝子をもつ植物形質転換用バイナリーベクターの開発を行った。本ベクターシリーズでは既存のpGWBシリーズと同様の2種類のシステム（pGWBとR4pGWB）が取り入れられ、16種類のレポーターまたはエピトープタグも利用可能である。シロイヌナズナを用いた有用性試験の結果から本ベクターによる形質転換体は0.15 mg L^{-1}のツニカマイシンを含む培地によって最も効果的に選抜されることが示された。

以上の結果から、AtSec24Bと24CはCOPIIとして機能し、雌雄両方の配偶体形成に重複して関与していることが明らかにされた。また、開発されたツニカマイシン耐性バイナリーベクターはより多彩な多重形質転換体の作製に利用でき、今後の形質転換体を用いた植物研究の発展に貢献すると期待された。